MULTI-PLATFORM REMOTE-SENSING TOOLS FOR PEAT FIRE DETECTION AND MONITORING

Report

to the Water Research Commission

by

MAM Abd Elbasit[1], K Abutaleb[1], AT Grundling [1], M Chauke[1, 2]

[1] Agricultural Research Council
[2] University of the Witwatersrand

Report No. 2836/1/20
ISBN 978-0-6392-0205-1

November 2020

Obtainable from:

Water Research Commission

Private Bag X03

Gezina, 0031

South Africa

orders@wrc.org.za or download from www.wrc.org.za

EXECUTIVE SUMMARY

BACKGROUND

Peatlands are a rare and unique wetland type in southern Africa. The fact that they exist in water-deficit environments (where evaporation exceeds precipitation) makes them especially vulnerable to changes in the hydrology and water sources that sustain them in semi-arid countries like South Africa. Peatland ecosystem services range from carbon sequestration to water purification and hydrological regulation. They regulate water flow and enhance groundwater recharge. Apart from the fact that peatlands store over 30% of the world's terrestrial carbon, they also host 10% of the world's freshwater. Peatlands, in general, exist in areas with high water abundancy: high rainfall areas, such as the coastal areas of KwaZulu-Natal, the Eastern Cape and the Western Cape, as well as areas characterised by available groundwater such as primary aquifers in the coastal areas and karst systems of North West. Peat accumulates under permanently inundated conditions. Once the hydrological conditions change, peatland degradation begins.

Peat degradation can be categorised as either those resulting from naturally induced impacts (e.g. drought) or those resulting from anthropogenic factors, i.e. human-induced impacts (e.g. water abstraction). One of the oldest living mires (active growing peatlands) in the world is the Mfabeni mire in KwaZulu-Natal, which is 48,000 years old (Grundling et al., 2013). This shows that peatlands can adapt to climatic fluctuations over the years. However, with anthropogenic impacts on peatland systems, the degradation is usually rapid (i.e. it occurs over a short period of time) and has a high magnitude.

Peat degradation occurs when the water table drops. The peat then dries out, forms cracks and becomes oxidised due to its exposure to air. Peat degradation results in the release of CO_2 into the atmosphere, which contributes to climate change. This is the ideal condition for subsurface peat fires to occur. Peat fires can burn and smoulder for a long period of time, causing health risks to communities, their livestock and wildlife. Subsurface peat fires are difficult to detect with remotely sensed sensors and are characterised by lower temperatures than surface fires. Therefore, this project aims to develop a national multi-platform remote-sensing data system for a peat fire detection monitoring framework that integrates information from various remotely sensed and ground-sensed sources.

This final report gives an account of a two-year research project (1 April 2018 to 31 March 2020) on the methodology used, and research findings and conclusions of the respective activities aimed at developing a national multi-platform remote-sensing data system for a peat fire detection monitoring framework.

AIMS

This study focused on two aspects:

- The characterisation of peat moisture and thermal characteristics that affect the susceptibility of peat to fire
- The development of a national peat fire detection and monitoring framework for peatland management by integrating various data sources

RESEARCH APPROACH

The remote-sensing multi-platform peat fire detection and monitoring framework has been developed under the following guidelines:

- Provide comprehensive evaluation for the areas with high susceptibility to peat fire
- Provide an integrated methodology that can be technically developed for priority areas

- Provide a framework that is scale independent and can be extrapolated to cover the national scale
- Provide a framework with low initial and operational costs

METHODOLOGY

Peat fires are scale dependent. Monitoring techniques must therefore be dynamic in nature. Proposed data acquisition platforms were adapted to the required monitoring scale. On a national scale, the data sources used were the national database that relates to hydrological indicators, as well as time series data extracted at peat site locations. The second level is the field scale, which can be covered using moderate and high-resolution images. Additionally, time series for land surface indicators can be developed for an area at different locations and combined with spatially distributed indicators (maps). The third level is the local scale. At this level, affected areas need to be confirmed (i.e. if peat fires are active and to specify smouldering areas). This is a crucial step in risk management (e.g. to prevent entry, evacuate people and livestock, and for fire extinguishing and control purposes). The final step in the framework is to assess each component to understand the potential of the specific indicator in peat fire detection.

The monitoring framework has three major components, which correspond with different monitoring scales, ranging from national to local scales. These components are the groundwater level, soil moisture and wetting, and thermal emissions, and were assessed at three investigated sites: Lichtenburg, Molopo and Molemane in North West. The hydrological indicators, coupled with thermal information and vegetation indices, were used to assess peat system stress and dryness. Additionally, changes in the spectral and thermal signatures were assessed by placing a tray of moist peat on top of a hotplate (at 300 °C). The thermal and spectral changes in the peat were recorded every 30 minutes using a thermal camera and ASD field spectroradiometer.

Two field campaigns were conducted to characterise the level of degradation of the peat, specifically peat with susceptibility to combustion. The peat fires affected the three sites at different levels. Peat samples were collected from the three sites and stored at the Agricultural Research Council's Soil, Climate and Water (ARC-SCW) laboratories for experimental investigations. The soil moisture of the peat is a critical characteristic for its susceptibility to peat fires. An evaporation method was adopted to assess the water content of the peat using dielectric, thermal and optic methods. The soil moisture was monitored daily using moisture sensors, thermal analysers and a field spectroradiometer. At the same time, three core samples (100 cm^3) were collected from the peat samples after measuring the samples with each sensor to determine the moisture gravimetrically. The core samples were oven dried and used as reference values for soil moisture content (gravimetric water content). The gravimetric water content was then converted to volumetric water content using the bulk density of the peat so that it could be used as a moisture reference. Additionally, two peat fire experiments were carried out using a ceramic coil igniter and hot plate. The heat emission and distribution were monitored using a thermal infrared camera.

Two sites (Molopo and Molemane) were considered for unmanned aerial vehicle (UAV) applications to detect thermal anomalies and wetting levels. Two sensors were mounted on a hexacopter drone to capture multispectral (four bands) and thermal data. Thermal data was captured early in the morning to remove the sun-heat background and to detect any underground thermal emissions present. The multispectral data was captured in the middle of the day. The multispectral images were mosaicked, orthorectified and then resampled to 0.05 m resolution. The thermal data was calibrated using the ground control point temperature data. The thermal images were resampled to 0.08 m pixel size. Ground data, such as a surface spectral signature, was also captured using an ASD4 field spectroradiometer, soil moisture was captured using a dielectric sensor, and soil thermal characteristics were captured using a KD2 Pro thermal properties analyser. Various indices were calculated, such as the simple ratio (SR), Normalised Difference Vegetation Index (NDVI) and vegetation Red Edge Index (REI). A combined index was also calculated to determine the surface moisture, which is a major indicator for the susceptibility of peat fires.

RESULTS AND DISCUSSION

The three components that were investigated (groundwater level, soil moisture and wetting, and thermal emissions) gave the following results: Peat soil moisture can be effectively monitored using dielectric sensors with high accuracy. For accurate measurements, sensors need to be recalibrated as they are mainly calibrated for mineral soils. The thermal properties of the peat samples have significant association with the peat moisture. This association can also be used to evaluate the peat moisture level at different scales. Peat fires have a series of complex processes that affect the accuracy of small-scale laboratory simulations. The rate of the peat fire is very slow and highly affected by the peat moisture. Gases emitted during peat fires are expected to contribute to the rate at which the peat fire spreads. Cracks that form on the peat during the drying stages contribute to the oxygen increase in the lower layers.

At the two sites (Molopo and Molemane) where the UAV application was applied to detect thermal anomalies and wetting levels, the following results were obtained: The two sites showed vast differences in terms of vegetation distribution and wetting levels. The Molemane site (which was a less disturbed/healthier site) was compared to the Molopo site (which was a highly disturbed site). Peat saturation was found to cover a large area of Molemane due to high groundwater levels. However, neither site showed any underground thermal emissions with the thermal sensor. The thermal data showed a clear pattern for underground water distribution, which can be considered as another indicator for water levels of the peat system. The results for the Molopo site indicate confirmed areas with a reduction in wetness levels below saturation and thermal emissions.

KEY MESSAGE

Peatlands are under increasing threat from agriculture, mining and infrastructure development. Authorities should take extra precautions to prevent peat degradation and peat fires, which can occur underground. Peat fires are of major concern, especially in the timber industry, and an urgent request for a peat fire workshop was aired. The aim of such a workshop would be to bring authorities, environmentalists and the timber industry together to explain where and why peat fires occur, as well as to share the results of this study on how and if remote sensing could be used as an effective tool in natural resources monitoring and management. Wetlands, and specifically peatlands, are valuable natural resources that need to be electively monitored and managed. One of the needs expressed is how to control and rehabilitate peat fires in the short term and how to manage the problem in the long term.

CONCLUSIONS

The developed framework has various components that range from ground measurements to low-altitude sensors and satellite-based indicators. Peat fires are a set of complex processes and factors that interact with each other to make peatland systems susceptible to fire. The framework categorises the monitoring processes at three scales that range from the national to the local scale. At national scale, anomaly detection can be used to differentiate between healthy and degraded systems. This is done by analysing time series data that represents the land surface temperature, vegetation conditions and groundwater levels. The annual and seasonal analysis of the groundwater level showed a high association between groundwater levels and peat degradation levels at the three study sites. At single peatland system level, a moderate satellite resolution can be used to develop spatially distributed indices such as vegetation indices, land surface temperature and the Soil Moisture Index (SMI). Higher-resolution images (satellite or aerial-borne images) can be utilised to identify no-entry zones if fire is confirmed at the previous stages. The framework was tested at the three sites using time series and spatial indices. The validation stages are important for the framework’s indicators selection and for narrowing down. However, the above-normal rainy season affects the expected number of peat fire incidents across the country.

The UAV can provide detailed information about specific sites. However, due to the cost, monitoring the peatlands periodically using UAVs is not economically feasible. Field trips covered 60 ha over three days for the two sites, while image mosaicking and processing can take more than six days, depending on the area. Moreover, image storage (i.e. data storage) needs a great investment, which increases exponentially with every new product or calculated index.

RECOMMENDATIONS

The main aim of the study was to develop a national peat fire monitoring framework based on the integration of various data sources. Based on the research findings, the following recommendations and future prospects for research are made:

- The role of methane gas emission on peat fire processes and acceleration should be determined.
- The framework relies on peat "points" and peat "polygons". It is therefore necessary to have detailed studies that verify all peat sites and delineate these systems.
- Groundwater monitoring systems should be developed to update the peat monitoring framework with continuous and frequent groundwater-level data.
- An investment should be made in future research work to operationalise the framework at national or provincial level. The advantage of the operationalisation of the monitoring framework is to apply an automated peat fire monitoring system that automatically couples groundwater levels and anomalies detected from satellite-based information.
- It is suggested that the framework be hosted by the Department of Human Settlements, Water and Sanitation as the main custodian of ground and surface water information. However, the detection of peat fires can also be important for several directorates in the Department of Environmental Affairs, Forestry and Fisheries, and the Department of Agriculture, Land Reform and Rural Development.

ACKNOWLEDGEMENTS

The research team would like to thank the WRC for the financial support of this project on the development of multi-platform remote-sensing tools for peat fire detection and monitoring (Project No. K5/2836). We would specifically like to thank Dr B Petja and Ms J Penny.

The project team wishes to thank the following people for their contributions to the project.

Reference Group	**Affiliation**
Dr B Petja	Chairperson
Ms N Muthraparsad	Department of Water Affairs and Sanitation
Dr W Roets	Department of Water Affairs and Sanitation
Dr P Grundling	Department of Environmental Affairs: Legal, Authorisation and Compliance Inspectorate
Mr E Munzhedzi	Department of Environmental Affairs, National Resource Management: Working for Wetlands, North West
Mr J Bester	Department of Environmental Affairs, Forestry and Fisheries
Ms N Fourie	Department of Water Affairs and Sanitation

Others

Mr M Kidson	Agricultural Research Council – Soil, Climate and Water
Mr T Matema	Agricultural Research Council – Soil, Climate and Water (former laboratory manager)
Dr S Newete	Agricultural Research Council – Soil, Climate and Water
Mr H Weepener	Agricultural Research Council – Soil, Climate and Water
Mr E Economon	Agricultural Research Council – Soil, Climate and Water
Mr R Tswai	Agricultural Research Council – Soil, Climate and Water
Mr J le Roux	Agricultural Research Council – Soil, Climate and Water (Professional Development Programme student)

The research activities were conducted at three sites in North West, and we would like to thank all those who made this research possible:

- Lichtenburg Game Breeding Centre: Mr Neels Lourens (manager), who shared historic photographs
- Molemane Eye Nature Reserve managers: Mr Deon Dinale (former park manager) and Ms Patricia Molehe (current park manager)
- Neighbouring farm to Molemane Eye Nature Reserve: Mr Tinus Botha (owner)
- Molopo Private Park: Mr F Aucamp and Mr John Knox (owners), who shared historic photographs and areal videos

CONTENTS

LIST OF FIGURES

LIST OF TABLES

ACRONYMS AND ABBREVIATIONS

ARC-SCW	Agricultural Research Council – Soil, Climate and Water
ADE	Alpha-Derived Emissivity
ASTER	Advanced Spaceborne Thermal Emission and Reflection Radiometer
ATSR	Along-Track Scanning Radiometer
AVHRR	Advanced Very-High-Resolution Radiometer
GNDVI	Green Normalised Difference Vegetation Index
GOES	Geostationary Operational Environmental Satellite
LPWAN	Low-Power Wide-Area Networking
MODIS	Moderate Resolution Imaging Spectroradiometer
NDVI	Normalised Difference Vegetation Index
NDWI	Normalised Difference Water Index
NGA	National Groundwater Archive
NIR	Near-Infrared
NOAA	National Oceanic and Atmospheric Administration
NWGMP	North West Groundwater Master Plan
REI	Red Edge Index
RENDVI	Red Edge Normalised Difference Vegetation Index
SAIIAE	South African Inventory of Inland Aquatic Ecosystems
SMI	Soil Moisture Index
SR	Simple Ratio
SR_r	Red Simple Ratio
SR_{re}	Red Edge Simple Ratio
SWIR	Short-Wave Infrared
TIMS	Thermal Infrared Multispectral Scanner
TIR	Satellite Thermal Infrared
TISI	Temperature-Independent Spectral Index
ToA	Top-of-atmosphere (radiance or reflectance)
TVDI	Temperature Vegetation Dryness Index
UAV	Unmanned Aerial Vehicle
UNEP	United Nations Environment Programme

GLOSSARY

Peat is sedentarily accumulated material consisting of at least 30% (dry mass) of dead organic material (Joosten and Clarke, 2002).

Heat (thermal) capacity is the amount of heat to be supplied to a given mass of a material to produce a unit change in its temperature.

Thermal resistivity is a heat property and a measurement of a temperature difference by which an object or material resists a heat flow.

Thermal diffusivity is the rate of heat transfer of a material from the hot spot to the cold spot.

Thermal conductivity is the ability of material to transfer (conduct) heat.

Unmanned aerial vehicle is an aircraft without a human pilot on board (drone). The official name for a drone in South Africa is a “remotely piloted aircraft”.

CHAPTER 1: BACKGROUND

1.1 INTRODUCTION

Globally, peatlands exist in temperate environments (Figure 1.1a) and make up 50% of the world's wetlands (Grundling et al., 2017). Joosten and Clarke (2002) define a peatland as "an area with or without vegetation with a naturally accumulated peat layer at the surface", and peat as a "sedentarily accumulated material consisting of at least 30% (dry mass) of dead organic material" (Joosten and Clarke, 2002). Peat is partially decomposed organic material that accumulated under more or less water-saturated conditions resulting under anaerobic conditions (Rydin et al., 2013). The term "peatland" is used to encompass peat-covered terrain. The minimum depth of peat required for a site to be classified as peatland differs between 30 and 40 cm across different countries (Rydin et al., 2013; Martini et al., 2006). Vegetation growing on the surface deposits plant material such as leaves, stems and roots, which begin to decay, while new vegetation begins to grow on top of the deposited matter (Wieder and Vitt, 2006). Oxygen near the surface and root zone permits the new layers of vegetation to undergo humification. However, decomposition decreases dramatically for organic material below the water table due to saturation and anoxic conditions (Rydin et al., 2013; Wieder and Vitt, 2006). Peat accumulation rates vary across different peatlands, but are generally known to be in the order of 1 to 2 mm per annum (Lappalainen, 1996) or a few centimetres of vertical accumulation every hundred years (Rydin et al., 2013; Wieder and Vitt, 2006).

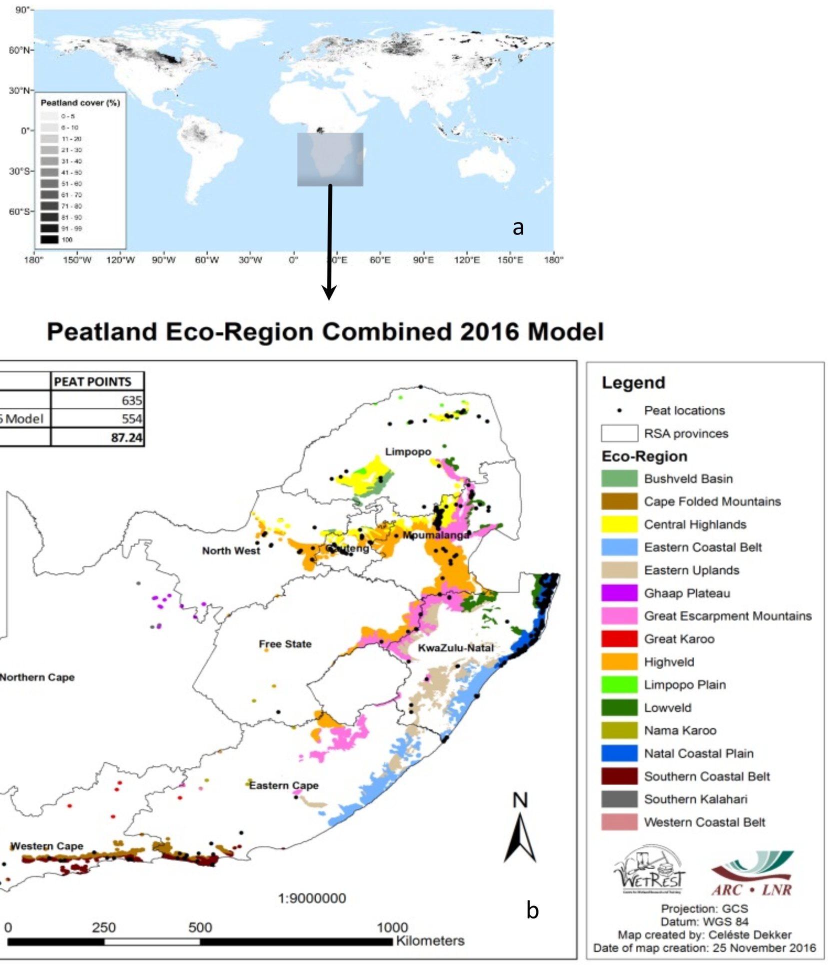

Figure 1.1: Peat soil distribution based on: (a) histosol data retrieved from HWSD v1.2 (after Xu et al., 2018); and (b) peatland ecoregions (Grundling et al., 2017)

South African peatlands are an exceptionally rare ecosystem type, as they account for less than 1.5% of the South African land surface. In South Africa (Figure 1.1b), peatlands cover approximately 300 km^2 of land (Marneweck et al., 2001; Grundling et al., 2017). Grundling et al. (2017) identified the most important peatland ecosystem services in South Africa. These are biodiversity, carbon storage and flow attenuation. Some 50% of South Africa's peatlands are found in the high rainfall areas of the Natal Coastal Plain Peat Ecoregion and in KwaZulu-Natal. In South Africa's semi-arid province of North West, peatlands occur in karst landscapes (Highveld Peat Ecoregion), which depend on groundwater, making these ecosystems special. Wetlands, and specifically peatlands, depend on the hydrological processes in their catchments (Holden and Burt, 2003). A change in any of these hydrological parameters, coupled with changes in land-use activities in the catchments, could significantly impact on and further degrade wetlands and peatlands (Grundling et al., 2017). Peat accumulation rates are slow, varying between between 0.5 and 2 mm per annum in South Africa (Grundling et al., 2017). South Africa's small, but unique peatlands (e.g. the Palmiet peatlands) still accumulate peat and continue to store and sequester atmospheric carbon, playing an important role in climate change. Another example is the Mfabeni mire, one of the world's oldest peatlands (Grundling et al., 2017). Estimates of the carbon accumulation rates range between 2,500 and 45,000 tonnes of carbon per year (Grundling et al., 2017). It can take thousands of years for a peatland to accumulate, but a matter of hours for it to be destroyed and greenhouse gases to be released, changing these systems from sinks to sources of greenhouse gasses (Joosten, 2010.). This can occur when fires in peatlands release the carbon contained in the peat by oxidising it into carbon dioxide. The bulk density of peat is one of the physical characteristics of peat that has an important impact on peat fires' rate of spread and emitted gases. The bulk density of peat can change due to the maturity and degree of decomposition of organic material. Additionally, changes in peat bulk density can occur due to a change in the moisture regime (Anshari et al., 2010; Hooijer et al., 2012) and due to the peat fire where this leads to the breakdown of peat into smaller particles (Wijedasa, 2016).

The exact extent and depth of peatlands in South Africa is uncertain because of a lack of detailed inventory work for the country. The South African Inventory of Inland Aquatic Ecosystems (SAIIAE) reported that only 169 of the 635 known peatland points in the National Peatland Database are represented in National Wetlands Map 5 (Van Deventer et al., 2018). The information used to compile the SAIIAE included some areas that were investigated infield with mostly point sampling and limited mapping of the peat extent or volume. These areas include parts of karst landscapes (in North West and Gauteng), the moist Highveld and escarpment (in Mpumalanga and the Free State), the KwaZulu-Natal coastal plain (Maputaland) and parts of the Cape Fold Mountains (in the Eastern Cape and Western Cape) (Grundling et al., 1998; Grundling and Marneweck, 2000; Grundling and Marneweck, 1999; Sliva and Grundling, 2002; Grundling and Grobler, 2005; Van Deventer et al., 2018). Yet, these unique ecosystems are being lost due to mismanagement (i.e. no monitoring framework and an unclear response strategy from government departments and landowners to prevent and stop peat fires). The aim of this report is to focus on the development of a fire detection framework for peat fire management.

1.2 PEAT FIRES

Peatland fires mostly occur in the upper metre of the peat as it is dry and flammable due to the extensive network of desiccation cracks and/or man-made drainage systems (Elvidge et al., 2015). The ideal condition for peat fires to occur is when the water table drops, causing the peat to dry out and form cracks, subsequently exposing the peat to air. Peat fires originate on the surface, and then spread downwards, unpredictably and slowly, as they are not affected by wind (Adinugroho et al., 2005). Fires in peatlands tend to fall within a fire's smouldering phase. Once ignited, they continue to burn for several days or even weeks. They smoulder beneath the surface, burning organic matter without any flames. White smoke is the only visible sign above the surface (Siegert et al., 2004; Elvidge et al., 2015; Adinugroho et al., 2005).

In the past two decades, various peat fires were reported in South Africa (e.g. the subsurface peat fire of the Lichtenburg peatland in the Harts River Catchment of North West) (Grundling and Marneweck, 2000; Grundling, 2018). These fires correspond to quarterly catchments where water abstraction takes place. Direct water abstraction includes agriculture (e.g. Bodibe in North West and the Sandveld in the Western Cape) and municipal activities (e.g. Molopo in North West for the water use of the town of Mahikeng). Indirect water abstraction activities, however, include commercial Eucalyptus and Pine plantations, such as at Lakenvlei in Mpumalanga and KwaMbonambi and Manzengwenya in KwaZulu-Natal, and gold and limestone mining, which impact on the peatlands of Molemani, Bodibe and Molopo, for example (Grundling and Marneweck, 1999). Grundling and Blackmore (1998) reported that long-term subsurface fires pose a threat not only to the local communities (e.g. air pollution and safety), but also to their livestock and wildlife. Local municipalities and landowners are ill equipped to extinguish the fires due to the danger and cost involved. Unfortunately, this situation was exacerbated during the drought (Malherbe et al., 2016; Malherbe et al., 2020) with more fires occurring during 2015 and 2016.

It is often difficult to extinguish a peat fire. It is thus important to detect them, determine their magnitude (i.e. area and intensity) and extinguish them before they reach dramatic, uncontrollable dimensions (Siegert et al., 2004; Adinugroho et al., 2005). Some studies have identified remote sensing as a potential tool to detect and monitor peat fires (Siegert et al. 2004; Elvidge et al. 2015; Gumbricht et al., 2002). This study seeks to evaluate the potential of identifying peat fires on the Molopo River System (North West) by developing a peat fire detection methodology based on integrated remote sensing technologies. At low altitude, ground sensors and satellite images will be considered. Peat moisture conditions will be used to detect the critical peat moisture levels that make the area susceptible to fire ignition and spreading.

1.3 PEAT FIRE MONITORING

The high accumulation of organic material in peatlands makes it highly vulnerable to fire when dry conditions prevail. Considering that peat fires occur below ground with a smouldering process and smoke appearing at the surface, attempts to extinguish them are often difficult. Peat fires can continue for long periods, ranging from a few weeks to several years, causing large amounts of harmful gas emissions (Filkov et al., 2015). Smouldering peat fires can spread on the surface and downward. The dominant underground peat fire is a dangerous type of fire for both local and firefighter personnel. The top unburnt peat can easily collapse.

Although peat fire processes have been accepted in the energy disciplines of science as a combustion process, the process is a result of hydrological changes in the peatland area. Due to peatlands being permanently saturated, the major hydrological characteristic of peatland is the positive hydrological status, where the storage component is usually a positive sign in the water balance equation (Whitfield et al., 2009) (Equation 1.1):

$$\Delta S = (\mathrm{P} + \mathrm{SW_{in}} + \mathrm{GW_{in}}) - (\mathrm{ET} + \mathrm{SW_{out}} + \mathrm{GW_{out}}) \qquad (1.1)$$

where ΔS is change in water storage (in soil or groundwater), P is direct precipitation, SW_{in} and GW_{in} are surface water and groundwater inflow (runoff, stream flow or subsurface flow), SW_{out} and GW_{out} are surface water and groundwater outflow, and ET is evapotranspiration (evaporation from plate and soil surfaces). The same equation is graphically elaborated on in a simplified way in Figure 1.2, which illustrates the water balance difference in a degraded peatland system as opposed to a pristine one.

In a basic peatland hydrological setup, the inflows are greater than the outflows and system losses. Most South African peat systems can be classified as minerotropic, where most of the water that enters the system is either from underground or stream sources (Grundling and Grobler, 2005). The three peatland systems investigated in this project receive their water from dolomitic eyes. Changes to the groundwater systems in these karst areas have affected the water yield in the respective dolomitic eyes, and thus lead to different degrees of severe degradation in the peat areas (DWAF, 2010).

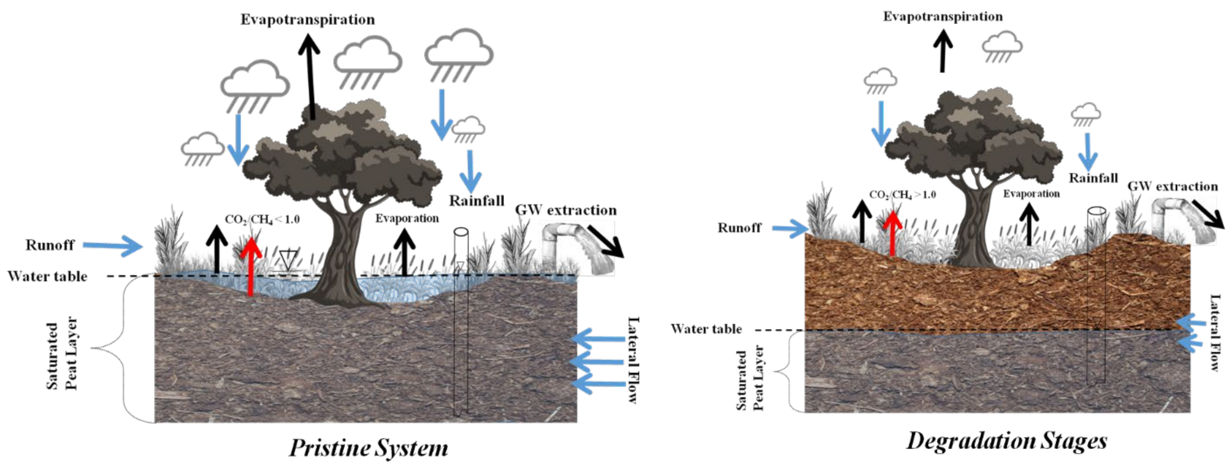

Figure 1.2: A peatland hydrological setup under pristine and degradation stages

The water table and surface moisture (ΔS) of peatland are crucial components in the water balance that can indicate the level of degradation that the system is experiencing. These components can be considered as a starting point to monitor peatland degradation, followed by various stages until smouldering occurs (Figure 1.3).

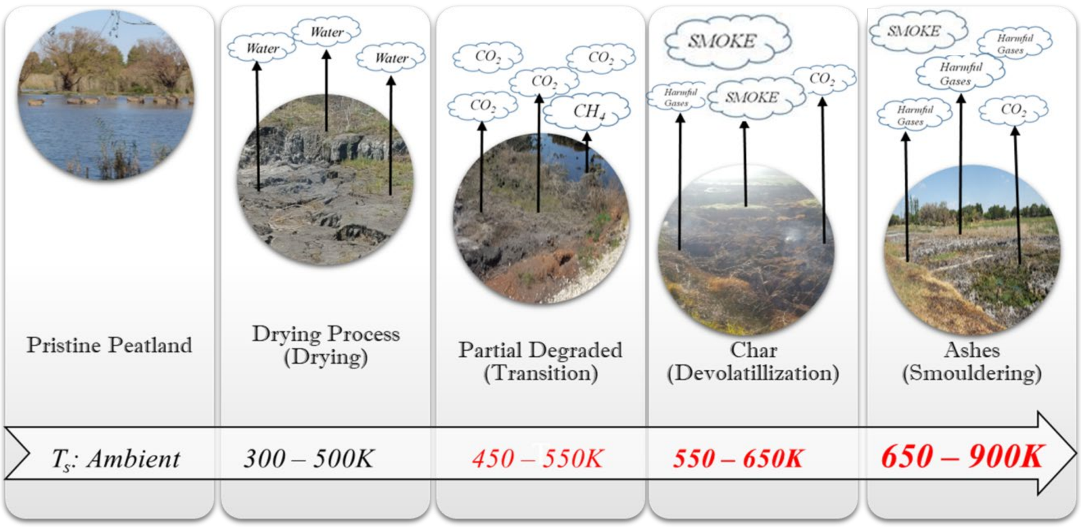

Figure 1.3: Simplified schematic view of peat fire processes and degradation stages (adapted from Cancellieri et al., 2014)

The degradation status of peatland can be monitored at each stage mentioned in Figure 1.3. Peat fires are difficult to identify because the smouldering stages occur under low temperatures compared to flaming fire processes, which can be detected using thermal remote sensing. Additionally, the rate of advance of a peat fire's front is highly related to the peat moisture and organic matter contents. The degradation processes can be noticed by changes in the ground water level of the peatland (Figure 1.2). The moisture depletion on the top peat layer can be considered an important stage because the peat loses most of its hydrophilic properties and undergoes a drastic reduction in its water-holding capacity. Water can then not be used to treat burning peat because the dry peat becomes water repellent (Perdana et al., 2017). At the stage of smouldering and devolatilisation (Figure 1.3), thermal indicators can be utilised to identify burning and non-burning areas. The thermal signature is quite small due to smouldering occurring at a low temperature and underground with a partially moist surface. For these reasons, peat fire detection and monitoring must utilise integrated approaches that are able to investigate peatland conditions at each stage of degradation to identify suitable restoration and conservation measures.

1.4 MOTIVATION

Peatlands are unique wetland types found in the semi-arid South African landscape (Grundling and Grobler, 2005). Although peatlands cover small areas, peat has various ecological services, which range from provisioning services (food, fresh water and genetic resources) and regulating services (water regulation and purification, and ground water recharge) to cultural and supporting services (Grundling et al., 2017). All these goods and services are lost in desiccated peatlands (Grundling and Blackmore, 1998). Peat fires can be considered as one of the consequences of peat dryness and have huge health, safety and environmental impacts, not only at local level, but at global level as well (Grundling, 2011). Peatlands are considered the largest terrestrial pool of carbon, and under conditions of degradation, release large amounts of carbon dioxide and other toxic gases into the atmosphere. Peat fires usually occur under smouldering combustion (flameless) and are quite difficult to detect visually (Adinugroho et al., 2005). Additionally, peat fires can be initiated by a weak source of heat and can spread by an average of 25 mm h^{-1} (Drysdale, 1998), depending on fuel and moisture conditions. Peat fires are difficult to extinguish; thus, the development of early detection and monitoring techniques is important to protect rural communities and peat areas as important natural resources.

1.5 TERMS OF REFERENCE

This project aims to develop a systematic peat fire detection and monitoring methodology that uses remotely sensed data captured at various platforms, ranging from ground monitoring to airborne (UAV) and space levels (satellite). This project considers three platforms: ground monitoring, low altitude sensors and satellite-based images.

1.6 RESEARCH APPROACH

The research approach is summarised in the following conceptual diagram (Figure 1.4). The ground-monitoring techniques used in this study were used as a validation source of information, while satellite-based monitoring was utilised as a continuous and low-cost source of information. The UAV was used at an operational level for high-resolution detection whenever the satellite showed suspected fire spots.

The current report is a series of experimental research activities aimed at developing baseline information based on the analysis of the historical groundwater level, peat moisture determination using a set of electrical, thermal and optical observations, and peat fire detection through thermal anomalies. The main challenge of peat monitoring is the underground smouldering fire processes. The direct application of thermal satellite data and conventional fire algorithms is therefore not applicable. Elvidge et al. (2015) summarised the difficulties in identifying smouldering peat fires based on the following factors:

- Peat burns and smoulders underground while satellites observe the surface.
- Fire detection algorithms often base detection in a single spectral band at 4 µm. It is impossible to distinguish between flaming and smouldering fires or to recognise pixels that contain both.
- Low temperature sources need to be detected. Large source areas are essential to yield sufficient infrared emissions.
- The smouldering nature of peat fires may result in the radiant emissions being dwarfed by the flaming phase emissions due to the absolute temperature to the fourth power in terms of the Stefan-Boltzmann Law.

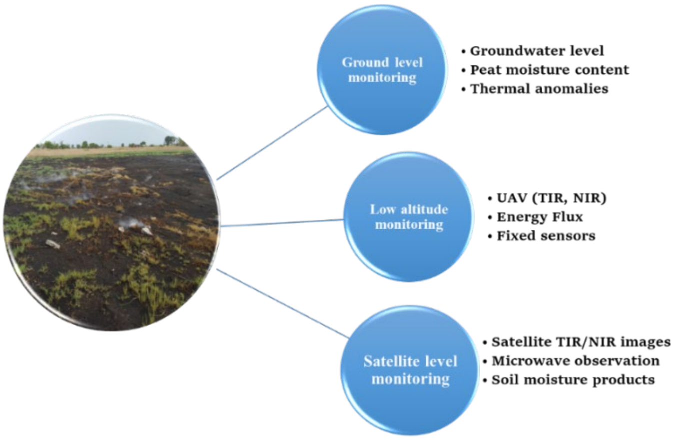

Figure 1.4: Conceptual diagram illustrating the research approach to developing multi-platform remote sensing tools and techniques for peat fire detection and monitoring

Detecting peat fires is challenging. The cause of peat fires could be lightning strikes or veld fires from adjacent areas that burn the dried peat. One of the major causes of dryness in peat areas is the lowering of the ground water level. Reasons for this include the excessive extraction of groundwater for domestic and agricultural uses. This also affects groundwater recharge by modifying the drainage system and land cover. An additional problem is that, after the surface fire, vegetation can re-establish itself on the surface of the peatland, but the peat could still burn and smoulder underneath where the depth of the fire will rely mainly on the water table. This fact has two major consequences. Firstly, peat fires can only be detected using thermal emission at an early stage, similar to flaming fires. Secondly, the location of underground fires will be difficult to determine using thermal data alone. Peat moisture/water content and ground water level characteristics have proven to have strong relationships with the ignition and spread of peat fires (Prat-Guitart et al., 2016). In this project, the integration of different remote sensing data generated at three levels (ground/low altitude sensor, drone (UAV) and satellite) will be used to determine the threshold thermal emission and moisture level for peat fire occurrence and the identification of areas with a high level of susceptibility to peat fires. Two work packages will be considered to achieve the above aims:

- The experimental determination of peat thermal and moisture relationships
- The development of an integrated multi-platform remote-sensing framework for peat fire detection

The results of the first work package will be used to determine suitable peat fire indicators that can be applied at different scales.

1.7 REMOTE SENSING APPLICATION

Every object emits energy proportionally to the fourth power of its surface temperature (Stefan-Boltzmann Law). The amount of energy emitted depends on the wavelength, i.e. as the temperature decreases, the maximum emission wavelength increases. In other words, the maximum detection wavelength becomes longer when the temperature is lower due to the minimum emission. For most of the land surface vegetation (between -20 and 50 °C), this maximum corresponds to a wavelength near 10 µm. Thermal infrared remote sensing has been proven to be beneficial in many environmental studies.

Thermal infrared has been utilised in studies of urban microclimates (Santamouris et al., 2001; Ngie et al., 2014; Abutaleb et al., 2015), water quality monitoring, vegetation stress (Sobrino and Caselles, 1991; Labbé et al., 2012; Stoll et al., 2008), fire detection and sea surface temperatures (Franca and Cracknell, 1994). Attempts to extract the land surface temperature from remote sensing data have been undertaken for just over a decade (Zhang, et al., 2006).

Remote sensing data supplies a practicable approach for the investigation of land surface temperature on wide spatial and temporal scales. Satellite thermal infrared (TIR) sensors measure top-of-atmosphere (ToA) radiances, from which brightness temperatures can be derived based on Plank's Law (Dash et al., 2002). The top-of-atmosphere radiance is the mixing result of three fractions of energy: the earth's surface emitted radiance, the atmosphere upwelling radiance and the sky downwelling radiance. At the exosphere (the outermost layer of the earth's atmosphere)/at the top-of-atmosphere (radiance or reflectance), the land surface brightness temperatures generally range from 1 to 5 Kelvin (K) (-272.15 to -268.15 °C) in the 10 to 12 μm spectral regions. These temperature differences depend on the atmospheric conditions (Prata et al., 1995). Therefore, atmospheric effects, including absorption, upward emission and downward irradiance reflected from the surface, have to be corrected before land surface brightness temperatures are obtained (Franca and Cracknell, 1994). These brightness temperatures should be further corrected with ground emissivity values prior to the computation of land surface temperature to account for the roughness properties of the land surface, the amount and type of vegetation cover, and the thermal properties and moisture content of the soil (Friedl, 2002).

Methods to retrieve land surface temperature depend on how the sensor's thermal bands were designed. One can classify satellites according to the number of thermal bands, which include a single thermal band such as Landsat satellites, two thermal bands such as the National Oceanic and Atmospheric Administration (NOAA), Advanced Very-High-Resolution Radiometer (AVHRR), Along-Track Scanning Radiometer (ATSR) and GOES (Geostationary Operational Environmental Satellite) satellites, and multiple thermal channels such as Advanced Spaceborne Thermal Emission and Reflection Radiometer (ASTER) and Moderate Resolution Imaging Spectroradiometer (MODIS) satellites. The split-window algorithms have been widely used for estimating land surface temperature from two thermal bands in the 10.5 to 12.5 μm region with given surface emissivity (Price, 1984; Sobrino et al., 1994; François and Ottlé, 1996). For multiple thermal band satellites, other formulae were developed to retrieve more accurate land surface temperature and emissivity from the satellite image itself. Among these formulae are the day/night algorithm, which is used for MODIS (Wan et al., 2002), the reference channel method (Lyon, 1965; Kahle et al., 1980), the Alpha-Derived Emissivity (ADE) method (Kealy and Gabell, 1990; Kealy and Hook, 1993; Hook et al., 1992), which is known as the alpha-residual technique, the Temperature-Independent Spectral Index (TISI) (Becker and Li, 1990; Watson, 1992), the optimisation algorithm and the ASTER algorithm (Liang, 2001; Gillespie, 1985; Realmuto, 1990; Li et al., 1999).

There are three basic modules in the ASTER algorithm: the normalised emissivity method, the ratio module and the maximum-minimum difference module. The main difference between the three modules is the methods used to estimate ground emissivity from the ASTER image. Numerical simulations show that the ASTER algorithm can estimate land surface temperature to within an error of 1.5 K and emissivity to within 0.015 (Gillespie et al., 1998). However, Dash et al. (2002) have previously reported that the algorithm requires an accurate atmospheric correction. Running ASTER algorithms on airborne multispectral thermal data applied this algorithm to the thermal infrared multispectral scanner (TIMS), which resulted in a land surface temperature with typical errors of 3 K (Schmugge et al., 1998). However, for satellites with a single thermal band, such as Landsat TM and ETM+, obtaining the land surface temperature is more difficult, as an accurate radiative transfer model is required, along with knowledge of the atmospheric profile and emissivity information (Qin et al., 2001). The most common methods adapted for retrieving land surface temperatures from the Landsat TM and ETM+ thermal data are the radiative transfer equation, the mono-window algorithm and the Jiménez-Muñoz and Soprano's algorithm (Sobrino et al., 2004). The first method requires *in situ* measurements of atmospheric data simultaneously with the satellite pass, which, in turn, may be a constraint for using this method. Meanwhile, the second and third ones could be used in the absence of this data, which uses the Normalised Difference Vegetation Index for calculating ground emissivity.

CHAPTER 2: RESEARCH METHODOLOGY

2.1 INTRODUCTION

The research project considered three sites that have been affected by peat fires at different times with various degrees of burning. The three sites are located in North West in the Lichtenburg, Molopo and Molemane areas (Figure 2.1). The three sites rely on dolomitic eyes (springs) for their water influx. The major characteristic for the peat systems in North West is the strip shape following the river valleys (Figure 2.1).

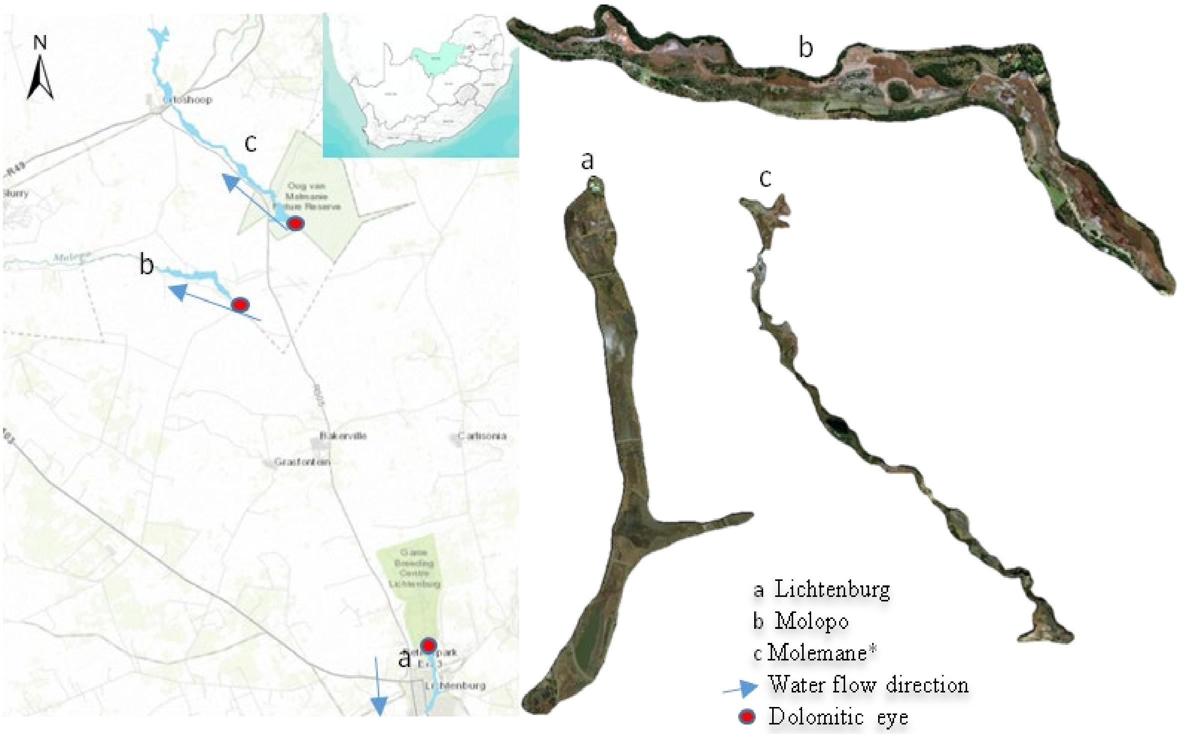

Figure 2.1: Locations of the three study sites and dolomitic eyes in North West (Molemane has been found in the literature with different spellings)

2.2 STUDY SITE INFORMATION

North West is South Africa's sixth-largest province in terms of surface area. The dominant landscape is grassland with semi-arid climatic conditions (Mucina and Rutherford, 2006). The province is well known for the rapid increase in mining and irrigated agricultural activities, and produces approximately 65% of the country's platinum. Climatically, North West can be classified between the arid and semi-arid environments (Figure 2.2a), where 78.3% is located within the semi-arid environment, while the rest falls within the arid zone, based on the common Aridity Index classification of the United Nations Environment Programme (UNEP) (1992). The average annual evaporation is 2,850 mm, while the annual precipitation varies between 200 mm in the northwest of the province to 700 mm in the eastern part of the province (Figure 2.2b) (Mucina and Rutherford, 2006). In general, the province has a total annual rainfall of approximately 539 mm, with the highest rainfall falling during the summer months of October and April (Bailey and Pitman, 2012; NWDACE, 2008). The province gets low rainfall during the winter months, with an average of 3 mm falling in July. The highest recorded 24-hour rainfall was 99 mm in the month of March (NWDACE, 2008). The annual evaporation (Figure 2.2c) varies from 1,900 to 2,700 mm per year and the vegetation cover (Figure 2.2d) mirrors the rainfall distribution (high in the east and low in the west).

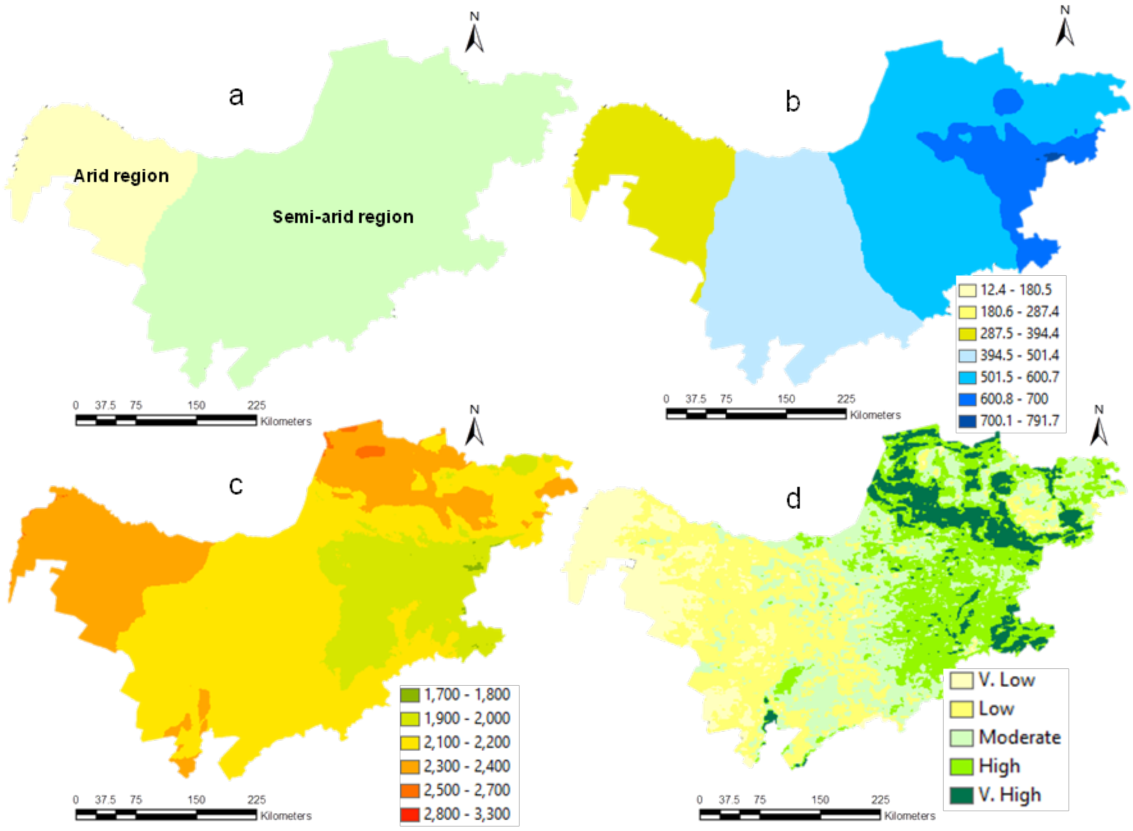

Figure 2.2: Climate characteristics of the study site: a) aridity; b) annual rainfall; c) annual evaporation; d) vegetation cover

The rapid increase in economic activity across the province has led to additional pressure on natural resources in general and on water resources in particular. The study sites are located within the karst belt hydrological region. Based on the North West Groundwater Master Plan (NWGMP) (DWAF, 2010), the aquifer can be classified as having between medium and high development potential, which creates high pressure on the region because of its suitability for domestic and irrigation water uses. The three peatland sites are located in a homogeneous geological formation (Figure 2.3a) and associated soil type settings (Figure 2.3b). The hydrological regime associated with these sites is the major driver.

2.3 SOIL MOISTURE DETERMINATION

The cracks that result from the desiccation of peat can be 0.2 to 0.5 m wide, and 1 to 3 m deep (peat blocks of 2 to 3 m wide will typically be separated by these cracks). A surface fire will often follow the dry rhizospheres of the burning vegetation and ignite the dry peat on the edge of the desiccation cracks. The fire will then spread along these cracks across the surface of the peatland, as well as downwards towards the water table. If the fire is hot enough and if the drying of the peatland continues, the fire will drive out the moisture in the peat and will continue to burn out the blocks of peat between the cracks, while penetrating deeper peat layers (Grundling, 2011). Thus, peat moisture determination is very important to understand the peat fire processes and susceptibility.

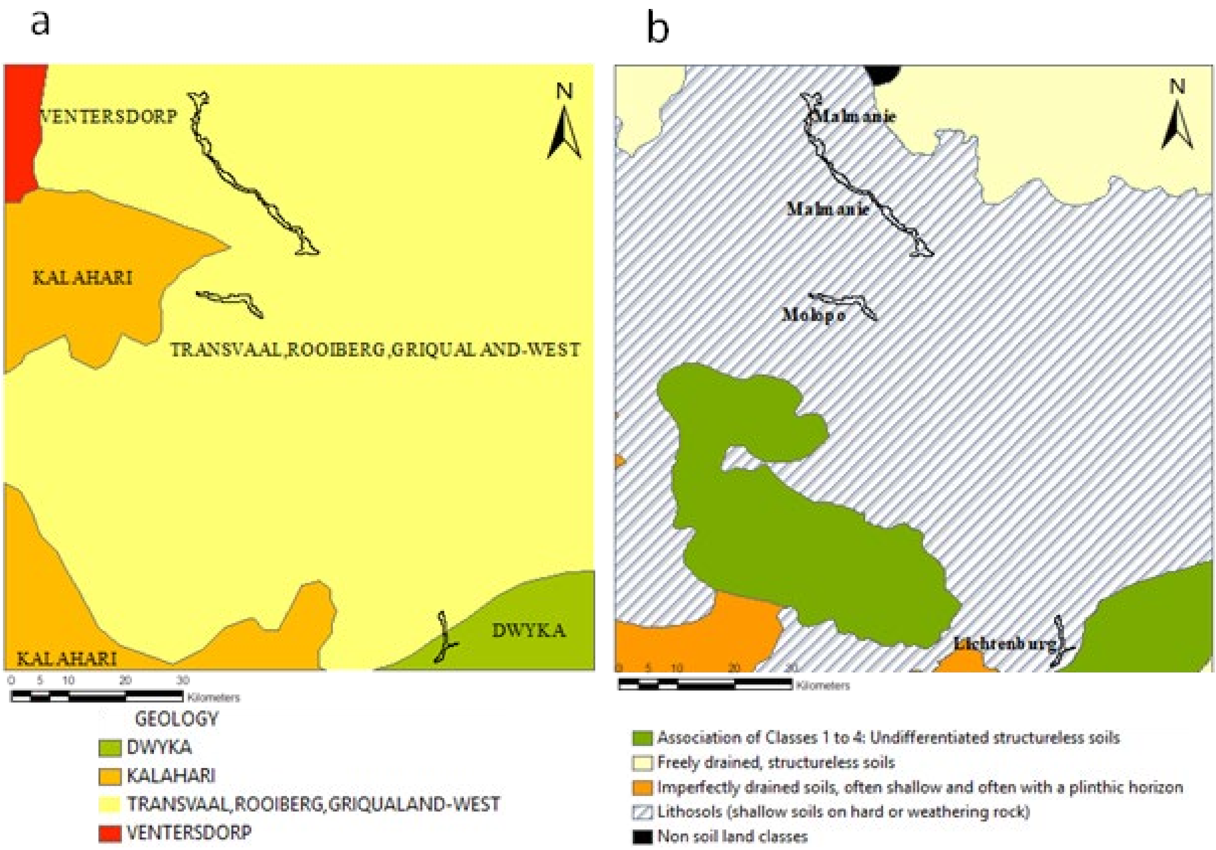

Figure 2.3: The three peat systems are located in a homogeneous setting in terms of: a) geology; and b) soil type

Two field campaigns were conducted to characterise the degradation of the peat level. The three sites, Lichtenburg, Molopo and Molemane, are affected by peat fire at different levels. The Lichtenburg site has been damaged by fire to a large extent. Moreover, the dolomitic eye that was supplying water to the system has dried completely, leaving a degraded system (figures 2.4a to 2.4d). The Molopo site has also been damaged by fire, but the eye is still supplying water to the system. The Molopo system lost its peat layer, leading to the development of new boundary conditions for the land surface (due to the drop in the land surface) and water started to appear on the new ash surface (figures 2.5a to 2.5c).

Figure 2.4: The Lichtenburg degraded peat site indicating: a) the depth (80 cm) of a crack with a peat auger; b) terrestrial and alien invasive vegetation colonising the once healthy peatland; c) the bare surface with ash on the surface (white); d) the ash core sample, which is very consolidated; and e) the core sampling procedure

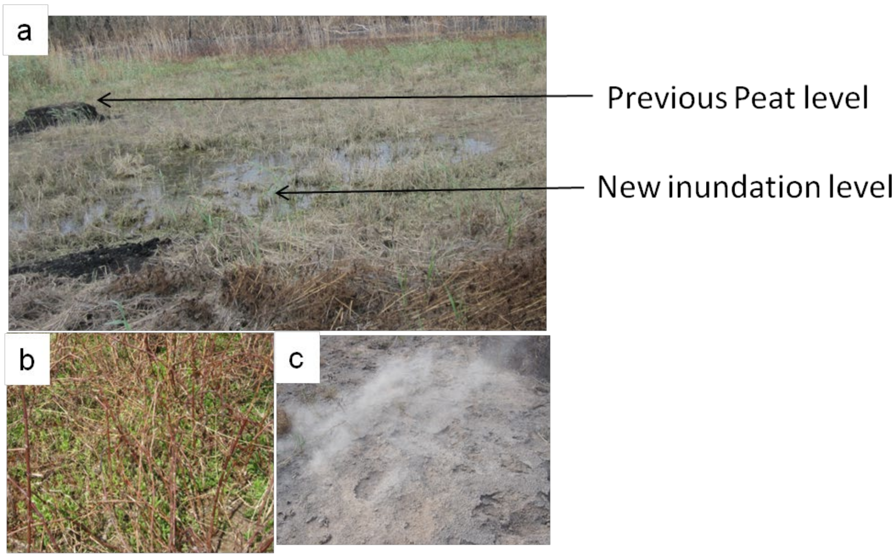

Figure 2.5: The loss of the peat layer in the Molopo system indicating: a) the previous peat level and inundation level; b) the new vegetation cover; and c) the dust of the peat ash, which can be considered a health hazard for locals

The Molemane site has limited fire impacts, as the fire only affected the southern part (figures 2.6a to 2.6d).

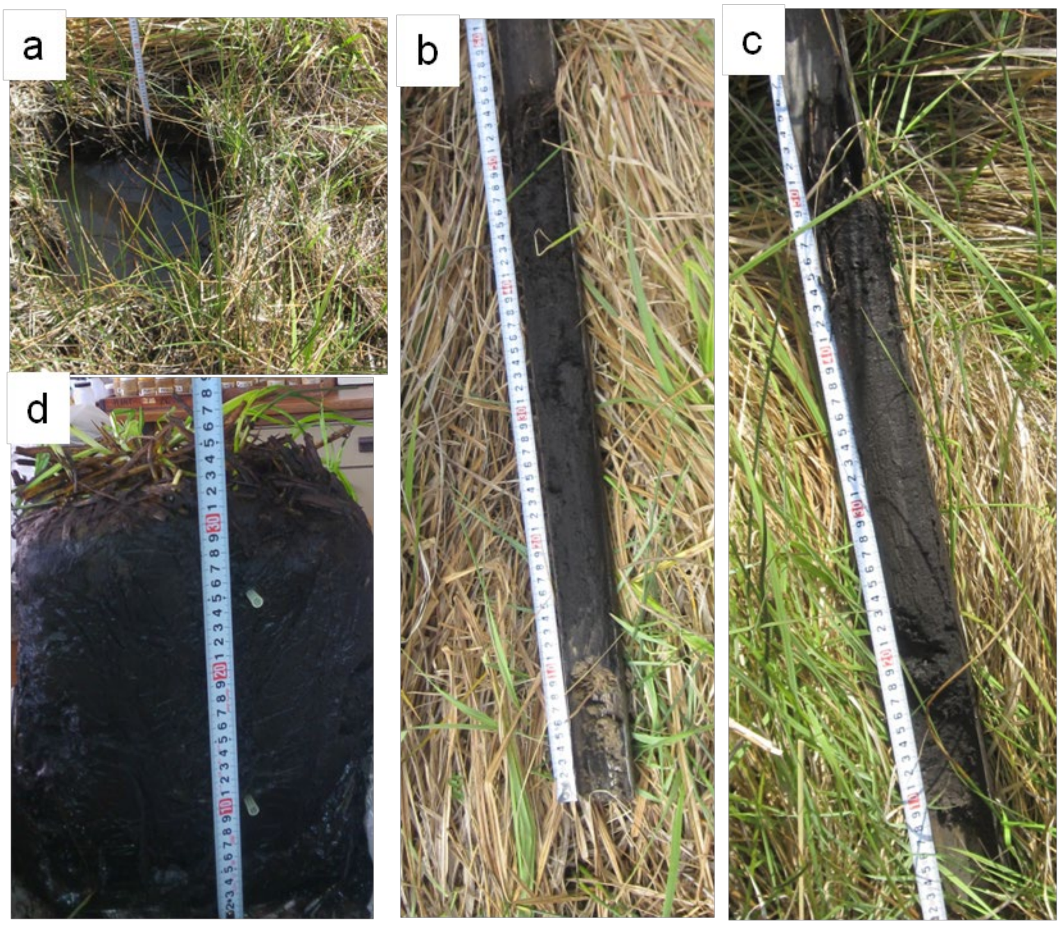

Figure 2.6: Peat sampling was conducted at the Molemane site: a) the high water table; b) the peat core sample at 20 m from the water body; c) the peat core sample at 10 m from the water body; and d) 30 cm, which indicates the peat block (undisturbed) sample

Peat samples were collected from the three sites and stored at the ARC-SCW laboratories for experimental investigations. Since peat soil moisture is a critical characteristic for fire suitability, conventional soil moisture methods were used to determine gravimetric water content after oven drying of the peat sample. However, the method is destructive and does not provide rapid results. Different types of soil moisture sensors can be utilised to evaluate the peat moisture at field level. However, due to the high organic matter content of the peat, the sensor was recalibrated to the peat's different levels of mineral content. For the sensor's calibration, known moisture samples were prepared and measured using different sensing methods.

Various methodologies can be utilised to prepare soil samples with different moisture content levels for the calibration of the sensors. However, peat characteristics, such as water-holding capacity, change drastically with dryness. For this reason, an evaporation method was adopted to assess the peat's water content using dielectric, thermal and optical methods. Fresh peat samples were collected from the field. The sample was placed in an aluminium tray with width, length and depth dimensions of 30 x 50 x 20 cm (figures 2.7a to 2.7d). The thermal properties of peat soil under different moisture levels were measured using a KD2 Pro thermal analyser.

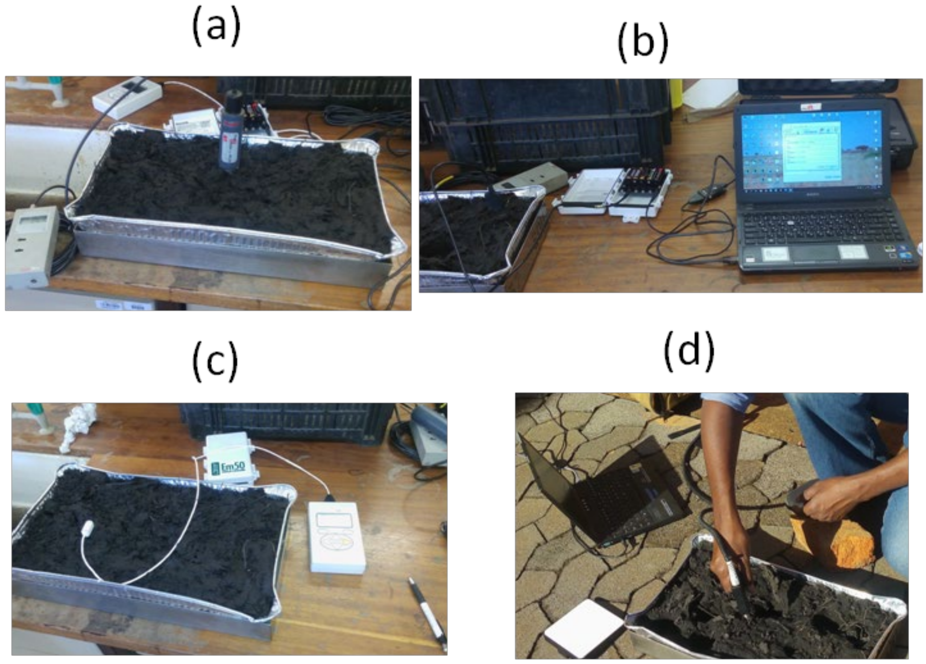

Figure 2.7: Peat moisture experiment and observations: (a) Theta probe; (b) 5TE volumetric moisture sensor; (c) KD2 Pro thermal analyser; and (d) ASD peat reflectance measurement

The aluminium tray was perforated to allow free drainage for the gravity water. The sample was then saturated for 24 hours using a similar metal tray filled with tap water and then removed from the water and left for 12 hours to drain the excess water. The tray was then left at room temperature, except for the last two days, when the samples were oven dried, and the soil moisture was monitored daily using moisture sensors, a thermal analyser, and an ASD field spectroradiometer. The field spectroradiometer is a device that collects the spectral reflectance of objects in the spectral range of (350 to 2,500 nm). The ASD 3 field spectroradiometer was used to collect the spectral reflectance of peat samples under different thermal and moisture content conditions. Four measurements were taken at exactly the same time each day for four consecutive days. Four replicates were captured for each peat sample. Three measurements were saved for each replicate, resulting in a total of 12 measurements for each single plot. The measurements were taken in the reflectance mode, which means that the ASD field spectroradiometer will measure the reflected energy from the surface under investigation. It was necessary to measure the incident energy from the sun to calculate the reflected percentage. For this purpose, the ASD white reference Spectralon® panel was used to calibrate the field spectroradiometer. Spectral files were pre-processed in the View Spec software and binary files were converted to ASCII text files so that processing could be carried out. The spectral signature files were opened and processed in R statistical software to calculate the average spectral value of each replicate, as well as the plot average. Three core samples (100 cm^3) were collected from the tray after each sensor's measurements had been taken, which were also oven dried and used as a reference for soil moisture content (gravimetric water content).

2.3.1 Peat bulk density

The bulk density for the Lichtenburg site was performed at the field level due to the cohesive nature of the ash and mineral material. However, due to the wetness and high ash content at the Molopo site, the bulk density measurements were performed at the ARC-SCW laboratory using a soil clod method. At the Molemane peatland, the bulk density was measured by sampling a 30 x 30 x 30 peat cube. The different layers of the peat were sampled using the 100 cc core sampler.

The 100 cc core was pushed into the peat block sample at different peat depths (Figure 2.7d). Vegetation at the upper part of the cube resulted in a major source of error in the core sampling. The gravimetric water content was then converted to volumetric water content using the sampled bulk density.

2.3.2 Utilisation of dielectric sensors

After the excess water of the samples had been drained, two dielectric constant sensors were used to measure the water content. The first sensor was a Theta probe connected to a direct reading module developed by Daiki, Japan (Figure 2.7), and the second sensor was a 5TE connected to an EM50 logger (Decagon) (Figure 2.7). Sensor readings were captured using ECH2O utility software.

2.3.3 Relationship between the peat's thermal characteristics and soil moisture

The thermal properties of the peat were measured using a KD2 Pro thermal analyser manufactured by Decagon, USA. The analyser consisted of two parts: the KD2 Pro keypad, and the SH-1 dual needle. This sensor was used to measure the volumetric heat capacity (MJ m^{-3} K^{-1}), thermal diffusivity (mm^2 s^{-1}), thermal conductivity (W m^{-1} K^{-1}) and thermal resistivity (C cm W^{-1}). The changes in the thermal properties have been associated with the peat moisture content. The thermal properties were measured on a daily basis (Figure 2.7c).

2.3.4 Remote-sensing applications

The peat surface reflectance was measured at different peat moisture levels using an ASD field spectroradiometer. This field spectroradiometer measures the reflectance at wave lengths that range from 350 to 2,500 nm. The peat tray was placed under sun illumination and white reference measurements were taken before the sample reflectance was measured. The reflectance was measured three times at four points (Figure 2.7d).

2.3.5 Experimental peat fire detection using thermal infrared

Peat fire processes are quite complicated. The fire occurs and spreads at a very low rate compared to flaming/surface fires. Surface fires rely on wind and fuel to spread, while peat fires spread under low oxygen conditions and spread by drying the peat at the advance line until it consumes all the organic material or encounters a high water content zone (saturated zone with continuous water supply). Considering all these conditions, the exact simulation of a peat fire at laboratory level is quite complicated. Thus, two fire experiments were performed to provide data to identify the peat moisture threshold for fire susceptibility and to monitor the heat energy emitted under a vegetated and a wet surface.

2.3.6 Experimental design

Two experiments were conducted to evaluate the performance of thermal imaging to monitor the progression of the peat fire. The first experiment considered the peat moisture levels with intermitted ignition, while the second experiment was used to evaluate the thermal anomalies on the surface using a constant temperature plate at the bottom of the peat. The thermal change on the surface was monitored using a thermal infrared camera. A ceramic coil heater connected to a thermostat switch was used to simulate heat igniting the peat. In natural conditions, peat fires initiate from weak pre-heating, which leads to smouldering processes (Prat-Guitart et al., 2016). The thermostat was used to regulate the peat's ignition area and avoid flaming. The ignition coil was then located on a ceramic plate connected to an electricity source and temperature sensor, all held in a 30 x 20 x 15 cm aluminium tray (Figure 2.8a). The tray was filled with peat at different wetting conditions. The peat's wetting conditions were controlled using different drying times in a convective heat oven adjusted to 70 ºC. The peat's moisture and thermal properties were measured before the fire experiments took place. The ignition was then started for five minutes and stopped, and the distributed temperature was measured using the thermal camera.

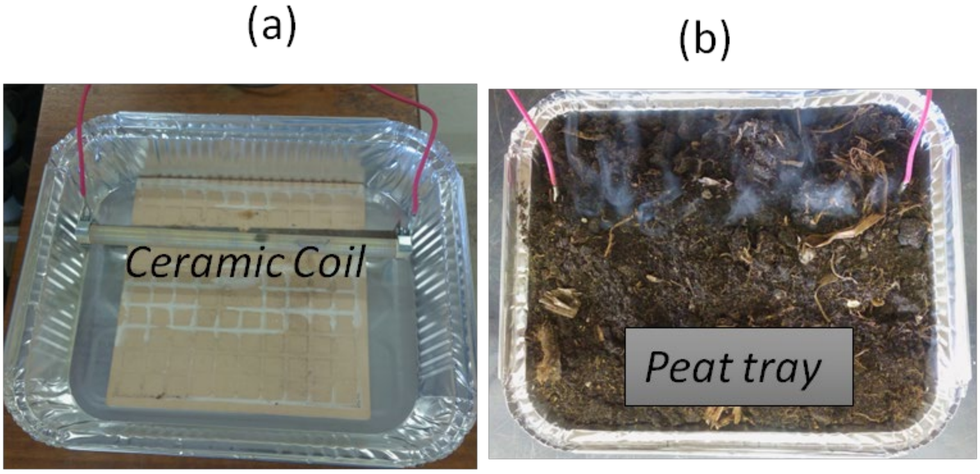

Figure 2.8: Peat fire experiment: (a) ceramic coil (ignition); and (b) peat fire aluminum tray

2.3.7 Data analysis

The association between the peat's gravimetric and volumetric moisture content on the one side and the sensors (θ and volt), thermal properties and surface reflectance on the other was determined using regression analysis. The method is also aimed at developing calibration equations for these indirect methods to effectively use the sensors at field level. The thermal images were analysed using a FLIR® Tool to extract the distributed temperature information.

2.4 EXPERIMENTAL PEAT HEAT DETECTION

The three research sites (Figure 2.1) have experienced peat fires with different levels of degradation. Currently, the three systems are not experiencing fires and it will not be possible to initiate fires in small areas for experimental purposes because of the possibility of the uncontrolled spread of these fires. Various scientists have reported peat self-ignition (e.g. Drysdale, 2011; Restuccia et al., 2017). The process occurs under carbon-rich soils due to spontaneous exothermic reactions with oxidative atmospheres and low temperatures (Drysdale, 2011). These reactions will not generate energy that raises the material temperature. The temperature increase is mainly related to the imbalance between heat rate generation and heat loss (Restuccia et al., 2017). The ignition in peat fires can occur from internal sources (self-heating) or external sources (e.g. lightning or flaming wildfires). In order to study the potential of spectral and thermal imaging in the detection of peat fires, a tray of fresh and wet peat has been placed on a top of a Labotec® hotplate (Figure 2.9). The hotplate had an adjustable temperature, and the temperature could rise to a maximum of 300 °C. The peat moisture and thermal characteristics were measured every 30 minutes from the start to the end of the hotplate experiment. However, because of the effect of the heat on the dielectric measurements (usually over-estimating the moisture), the measurements were stopped after three hours from the beginning of the experiment due to an increase in the peat's temperature. The peat's surface temperature and spectral reflectance were captured using a FLIR® C3 handheld thermal camera and ASD® Field Spec spectroradiometer, respectively (Figure 2.9). The thermal and spectral data were also captured every 30 minutes.

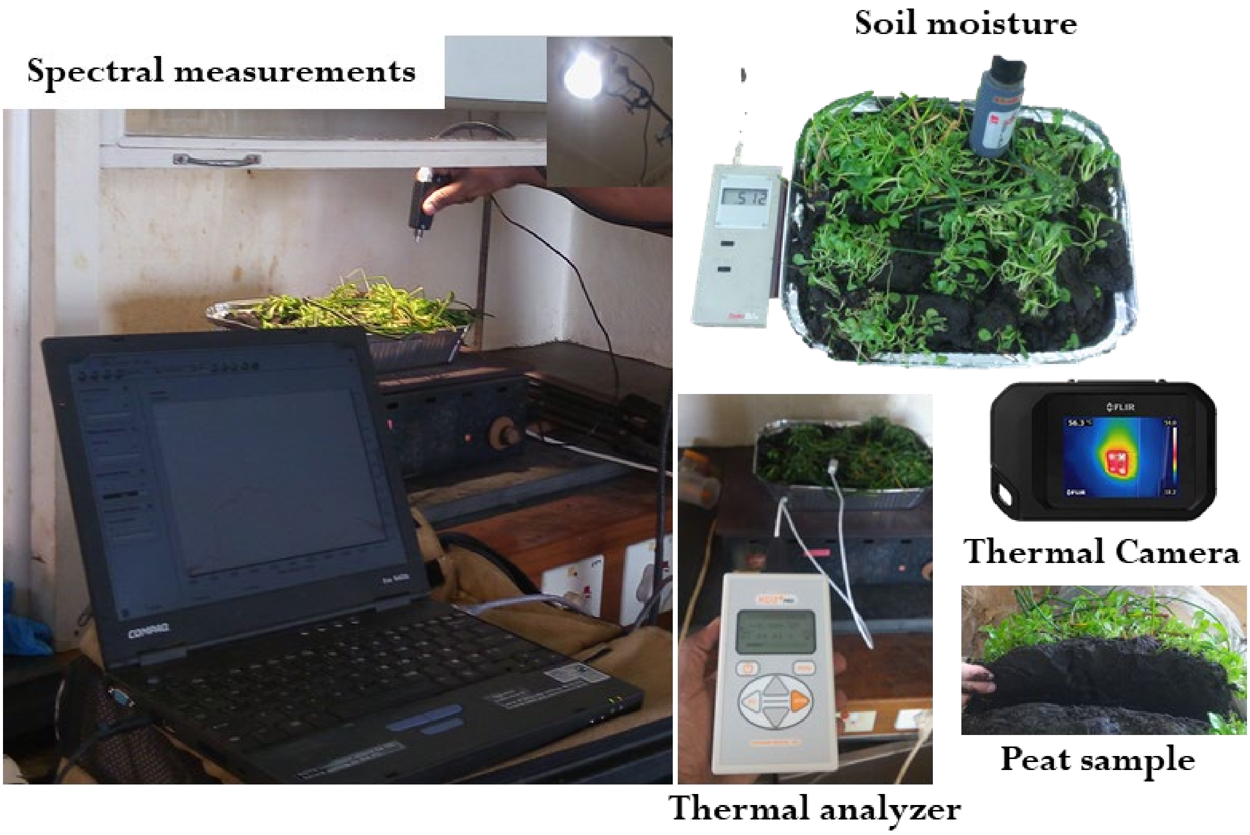

Figure 2.9: An experimental view of the peat heat detection and spectral data acquisition

2.5 GROUNDWATER LEVEL TRENDS

Based on Figure 2.10, groundwater is one of the major indicators of peatland degradation and defines the area's susceptibility to peat fires. Because groundwater level monitoring is a straightforward procedure, it has been included in the proposed detection and monitoring framework as a basic hydrological input, which can also be extrapolated to large areas with automatic data acquisition. Groundwater levels for the study sites were retrieved from the South African National Groundwater Archive (NGA). The NGA Tool is user friendly with various types of data. Seven stations are distributed within the karst system area in North West (Figure 2.11). Based on the lithological reports for the area retrieved from the NGA, the common lithology layers are dolomite, shale and vein-quartz.

Figure 2.10: Groundwater monitoring wells at the three investigated sites and satellite-based time series assessment polygons

2.6 SATELLITE-BASED TIME SERIES AND ANOMALY DETECTION

Landsat 7 and 8 images for the period 1999 to 2018 (270 images) were considered for long-term time series analysis. The pre-processing of the images included cloud image masking, radiometric corrections and the calculation of reflectance and radiance for the optical-infrared and thermal bands. Several indices were then calculated using different band combinations. The indices included surface temperature (T_s), the Normalised Difference Vegetation Index, the Soil Adjusted Vegetation Index and the Normalised Difference Water Index. Time series were extracted using different modes, such as the entire system average, subsystems and small polygons (Figure 2.10).

2.7 SATELLITE-BASED SPATIAL INDICATORS

The development of spatial indicators was suggested after confirming the degradation status of the respective peats, which was based on the ground water level and time series anomalies. Indicators were similar to the time series, as both were extracted from satellite data (Landsat 8). The indices have been classified into four major categories: vegetation indicators, water indicators, thermal indicators and combined indicators. The vegetation indicators included the Normalised Difference Vegetation Index, the Soil Adjusted Vegetation Index and the Green Difference Vegetation Index. The Normalised Difference Water Index was used as a water index from the short-wave infrared. The thermal indicators were calculated for the two thermal bands of Landsat. The combined indicators were aimed at utilising the thermal and vegetation indices to evaluate the plant stress, energy balance and soil moisture in spatial context. The data was masked for the three research sites (Figure 2.10)

2.8 UTILISATION OF UNMANNED AERIAL VEHICLES

The application of the UAV in high-resolution peat fire detection can be used at the third stage of peat fire confirmation to assist in the identification of smouldering areas. This technique can help protect the local community and act as guidance for firefighters at field levels. Multi-spectral and thermal data are suggested for the optical, thermal and combined indicators. The two proposed sensors were tested at indoor conditions (Figure 2.11). The multi-spectral data was captured using RedEdge-M™ produced by MicaSense®. The camera has five spectral bands: blue, centred at 475 nm (20 nm width), green, centred at 560 nm (20 nm width), red, centred at 668 nm (10 nm width), red edge, centred at 717 nm (10 nm width), and near-infrared, centred at 840 nm (40 nm width).

Figure 2.11: Multi-spectral camera checks at the laboratory

The multi-spectral and thermal sensors were handheld and tested at indoor and outdoor conditions to assess their performance and ability to extrapolate the data from the field scale using a drone platform. The spectral camera can give up to an 8 cm ground pixel size at a height of 120 m.

2.9 LOW-ALTITUDE SURVEY SITES

Two peatland systems (Molopo and Molemane) were selected for the UAV and ground surveys. The two sites represent different levels of degradation. The degraded site was the Molopo peatland, which had experienced severe peat fires between 2014 and 2016. The Molemane site can be considered a pristine system or system with minimum disturbance at the considered segment (Figure 2.12).

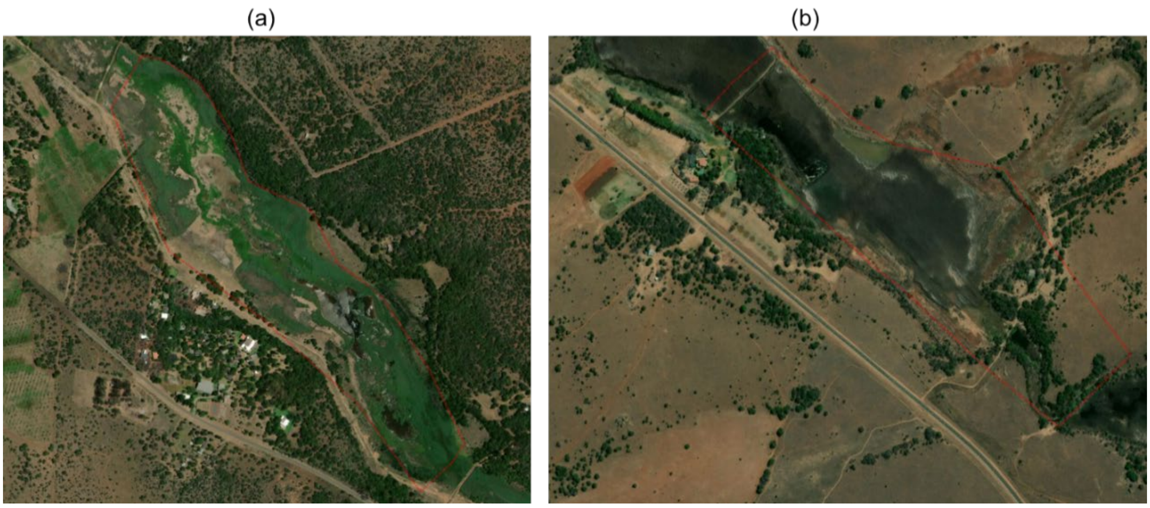

Figure 2.12: Location of the two UAV sites: (a) Molopo; and (b) Molemane

2.10 UNMANNED AERIAL VEHICLE MONITORING SYSTEM

Two sensors – multispectral and thermal sensors – were mounted on a DJI Matrice drone (Figure 2.13). The multispectral sensor used to capture the images (Table 2.1) was the Slantrange® 4P with four bands, which range between 410 and 950 nm. The four bands included green (520 nm), red (620 nm), near-infrared (820 nm) and red edge (670 nm). The ground resolution was 4.0 cm at 100-metre flying height. The areas of the Molopo and Molemane sites were 33 ha and 28 ha, respectively. The flight plan was arranged to cover a larger area (Figure 2.14). The thermal sensor was the FLIR® Vue Pro R with a 13 mm lens and a 640 x 512 sensor size (Table 2.2).

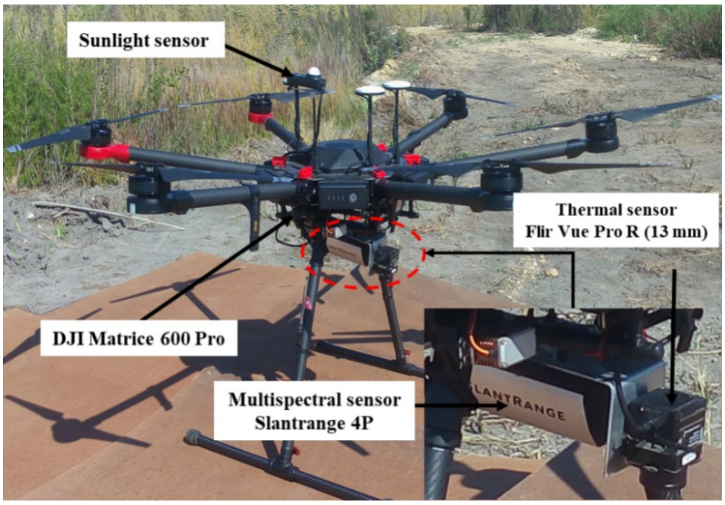

Figure 2.13: Unmanned aerial vehicle with available sensors utilised to monitor the peat conditions

Note: Specifying any brands and trademarks does not imply any endorsement or recommendation.

Table 2.1: Slantrange® multispectral camera specification

Characteristics	Specification
Spatial resolution (GSD @ 100 m AGL)	4.0 cm
Spectral channels	6
Available spectral range	410 to 950 nm*
Recommended image overlap	20%
Output formats	KML, SHP, GeoTIFF
Size	14.6 x 6.9 x 5.7 cm
Weight	350 g
Power	12 W @ 9.0 – 28.0 VDC

Table 2.2: FLIR® Vue Pro R thermal camera specification

Characteristics	Specification
Size	2.26" x 1.75" (including lens)
Spectral band	7.5 to 13.5 µm
Thermal imager	Uncooled VOx microbolometer
Weight	3.25 to 4 oz (configuration dependant)
Lens options	13 mm
Scene pre-sets and image processing	Yes – adjustable in app
Sensor resolution	640 x 512

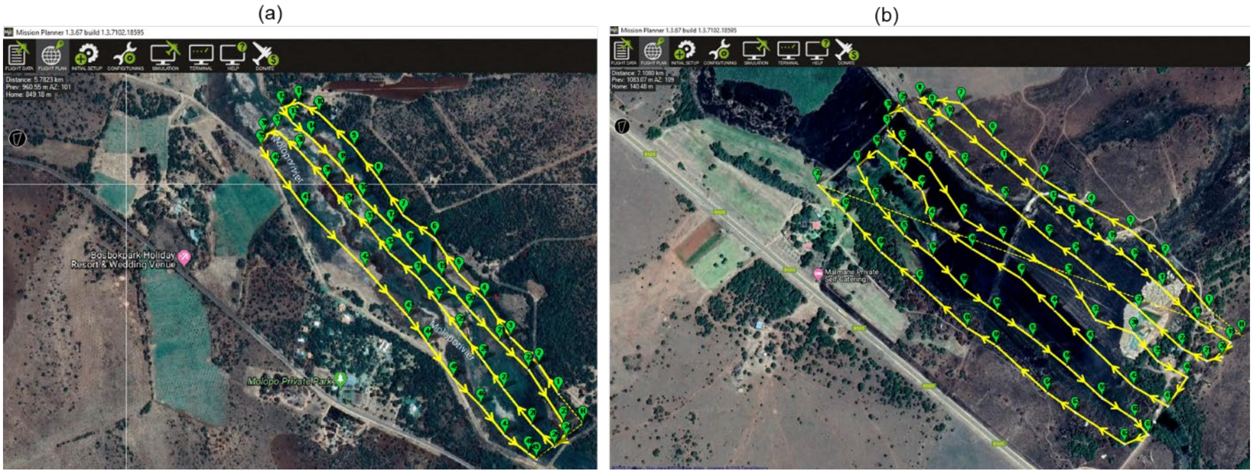

Figure 2.14: Flight plan for the: (a) Molopo; and (b) Molemane sites

2.11 GROUND DATA MEASUREMENTS

The peat moisture and thermal properties for the two sites were measured at different locations at the same time as the UAV survey, simultaneously. The peat moisture was observed using an ADR sensor calibrated at the ARC-SCW laboratory, as described in section 2.3 (Figure 2.15). The thermal properties were measured using a Decagon Pro thermal properties analyser (Figure 2.15).

Figure 2.15: Peat moisture and thermal properties monitored during the UAV survey

2.12 UAV IMAGES PROCESSING

The original resolution for the multispectral and thermal images was 0.05, and 0.08, respectively. Processing this resolution at the exploration and research stage was a very slow and memory consuming task. At the beginning, the UAV images were resampled to a coarser resolution of 0.5 m to allow for a variety of analysis techniques and peat fire indicators. Five indices were calculated (Table 2.3): Red Simple Ratio (SR_r), Red Edge Simple Ratio (SR_{re}), Normalised Difference Vegetation Index (NDVI), Green Normalised Difference Vegetation Index (GNDVI) and Red Edge Normalised Difference Vegetation Index (RENDVI). The indices were calculated using the resampled images (Table 2.3). A model was developed in ArcGIS (ESRI, 2020) to calculate these five indices (Figure 2.16).

Table 2.3: Spectral vegetation indices and formulae calculated using resampled UAV images

Name	**Index**	**Formula**
Simple Ratio	SR_r	$\frac{NIR}{R}$
Red Edge Simple Ratio	SR_{re}	$\frac{NIR}{RE}$
Normalised Difference Vegetation index	NDVI	$\frac{NIR - R}{NIR + R}$
Green NDVI	GNDVI	$\frac{NIR - G}{NIR + G}$
Red Edge NDVI	RENDVI	$\frac{NIR - RE}{NIR + RE}$

NIR = Near Infrared; R = Red; G = Green; RE = Red Edge

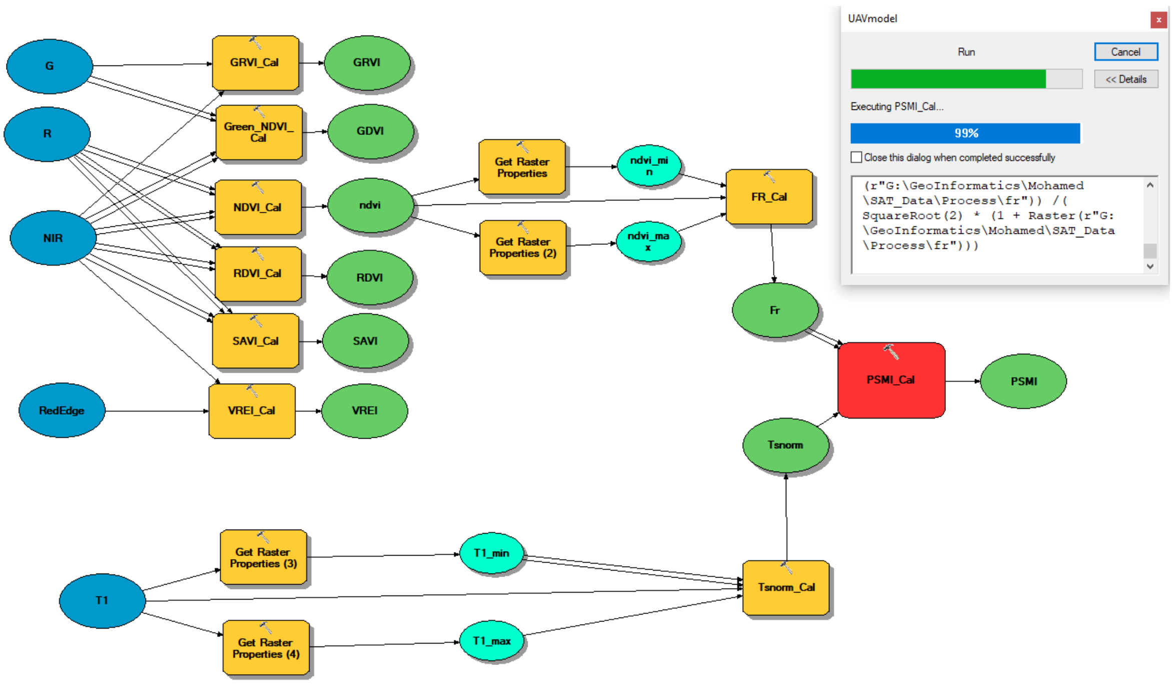

Figure 2.16: The ArcGIS model developed for indices calculations

2.13 DEVELOPMENT OF THE DETECTION/MONITORING FRAMEWORK

Peat fires have been proven to be highly related to changes in hydrological inputs. In other words, once the peat is dry, a fire becomes the subsequent result as soon as a source of ignition is found. Considering the water scarcity in the country, each peat system in South Africa is susceptible to dryness and fire. Keeping this in mind, peat degradation is a long process and requires continuous monitoring at national scale. Based on previous studies by Grundling et al. (2017), the locations of historical peat points are illustrated in Figure 2.17.

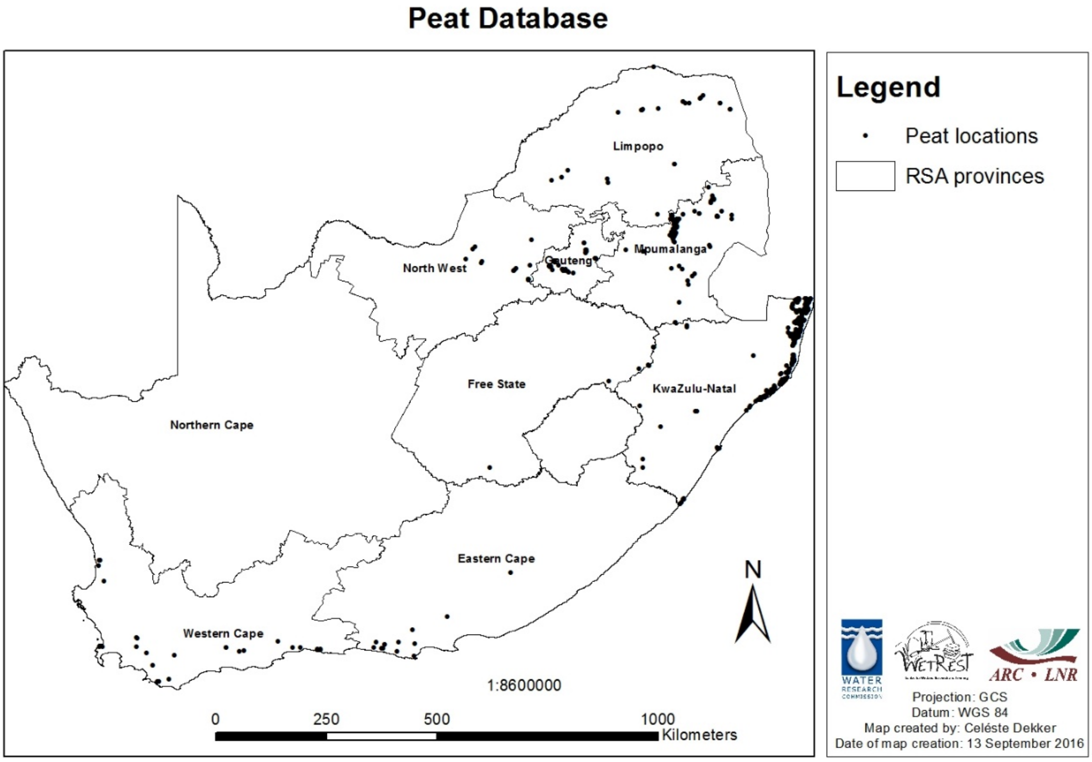

Figure 2.17: Known peat points from the National Peatland Database housed at the ARC-SCW (Grundling et al., 2017)

The detection and monitoring framework needs to fulfil the following major concerns:

- Provide comprehensive evaluation for areas with high susceptibility to peat fires
- Provide an integrated methodology that can be technically developed for priority areas
- Be scale independent and able to be extrapolated to cover the national scale
- Have low initial and operational costs

CHAPTER 3: RESULTS AND DISCUSSION

3.1 PEAT CHARACTERISATION AT THE THREE SITES

The extent of degradation at the respective peatlands was assessed by visually examining the remaining peat. The Lichtenburg site has been affected by fire to a large extent (Figure 2.4). Due the the depletion of the dolomitic eye, the peat dried, but did not necessarily burn. The change in peat surface elevation is one of the major signs of the loss of the peat layer, which was identified at the Molopo peatland (Figure 2.5). The Molopo peatland is covered entirely by a deep layer of ash (approximately 1.2 m), which can be considered an indicator for the burnt volume, and thus the amount of greenhouse gases that are released into the atmosphere. The Molemane site has been affected by peat fire on its edges with limited impact on the main system. The peat at the Molemane site is distributed unevenly across the peatland site (Figure 2.6).

3.1.1 Peat structure and level of degradation

The peat was structurally different at the three sites. This was confirmed by the peat's morphology, weight and composition. The bulk density of the peat was higher in the areas affected by peat fire or dryness (Figure 3.1). The highest peat bulk density was found at Molopo and Molemane at depths greater than 20 cm. The top peat layer at the Molemane site had the lowest bulk density due to the fibrous structure of the peat at this layer (Figure 3.1).

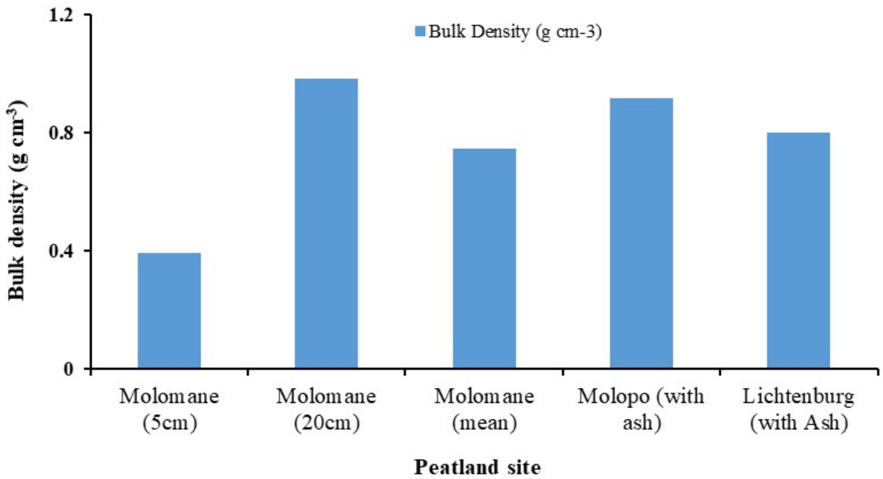

Figure 3.1: Peat bulk density at the three sites and different depths for the Molemane site

3.2 PEAT MOISTURE DETERMINATION

3.2.1 Utilisation of dielectric sensors for peat moisture

The peat's moisture was determined gravimetrically and volumetrically using 100 cm^{-3} core sampling (Figure 3.2). The core sampling in the peat was found to be challenging due to the existence of plant remains and roots, which can be considered to be among the major sources of error. The correlation coefficient between the peat's gravimetric/volumetric moisture content was calculated directly using the mass difference method. The dielectric sensors showed a high association between the peat measurements and the sensor outputs (Table 3.1).

Table 3.1: Correlation coefficients between the peat moisture content and dielectric sensor measurements

	W_v	**Volt**	**Theta**	**5TE**
W_g	0.928 (<0.001)	0.884 (<0.001)	0.885 (<0.001)	0.883 (<0.001)
W_v	1	0.969 (<0.001)	0.969 (<0.001)	0.968 (<0.001)
Volt		1	1.000 (<0.001)	0.972 (<0.001)
Theta			1	0.972 (<0.001)
5TE				1

W_g = Gravimetric moisture content; W_v = Volumetric moisture content; Volt = Volt output from the Theta probe; Theta = Output volumetric moisture from the Theta probe; 5TE = Decagon volumetric water, temperature and Ec sensor

The correlation results imply that using dielectric sensors has potential for the continuous evaluation of peat dryness. This can be used as an indicator of the level of degradation and fire suitability based on different organic and mineral content ratios. The regressed relationship between the volt on the one side and the W_g and W_v on the other (Figure 3.2) indicates the regression between the volt (Figure 3.2a) and the W_g and W_v (Figure 3.2b).

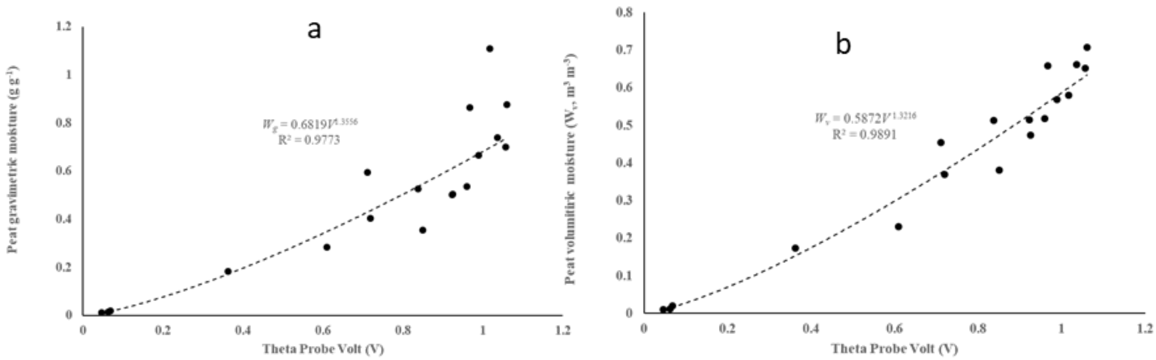

Figure 3.2: Relationship between the Theta probe output volt and gravimetric peat moisture

The sensor volt output was highly related to the volumetric moisture content compared to the gravimetric moisture. However, the results generally showed acceptable performance for the dielectric sensors in peat moisture evaluation with higher disturbance at wetter conditions. These results emphasise the importance of dielectric sensor calibration before it can be applied in peat moisture measurements.

3.2.2 Peat thermal characteristics and moisture content

The correlation coefficient between the thermal properties and moisture is shown in Table 3.2. The thermal properties showed significant association with peat moisture, except for thermal diffusivity. This result suggests that other factors may have a larger impact on thermal diffusivity than peat moisture. The thermal characteristics of the peat can also be used to determine peat moisture with higher sensitivity compared to the dielectric constant.

Table 3.2: Correlation coefficients between the peat's thermal properties and moisture content

	W_v	K	C	D	rho	T	W_g%
W_g	0.928 (<0.001)	0.702 (0.001)	0.871(<0.001)	0.165 (0.514)	-0.742 (<0.001)	-0.299 (0.299)	1.000 (<0.001)
W_v	1	0.818 (<0.001)	0.930 (<0.001)	0.308 (0.213)	-0.840 (<0.001)	-0.320 (0.196)	0.928 (<0.001)
K		1	0.910 (<0.001)	0.621 (0.006)	-0.903 (<0.001)	-0.185 (0.185)	0.702 (0.001)
C			1	0.311 (0.209)	-0.871 (<0.001)	-0.257 (0.303)	0.871 (<0.001)
D				1	-0.647 (0.004)	0.289 (0.245)	0.165 (0.514)
rho					1	-0.0845 (0.739	-0.742 (<0.001)
T						1	-0.234 (0.452)
Wg%							1

W_g = Gravimetric water content; W_v = Volumetric water content; K = Thermal conductivity; C = Specific heat; D = Thermal diffusivity; rho = Thermal resistivity; T = Peat temperature; W_g% = Percentage gravimetric moisture

3.2.3 Relationship between peat reflectance and moisture

The results of the ASD field spectroradiometer showed a clear increase in the entire spectrum, suggesting a clear impact of the dryness on the surface albedo (figures 3.3 and 3.4).

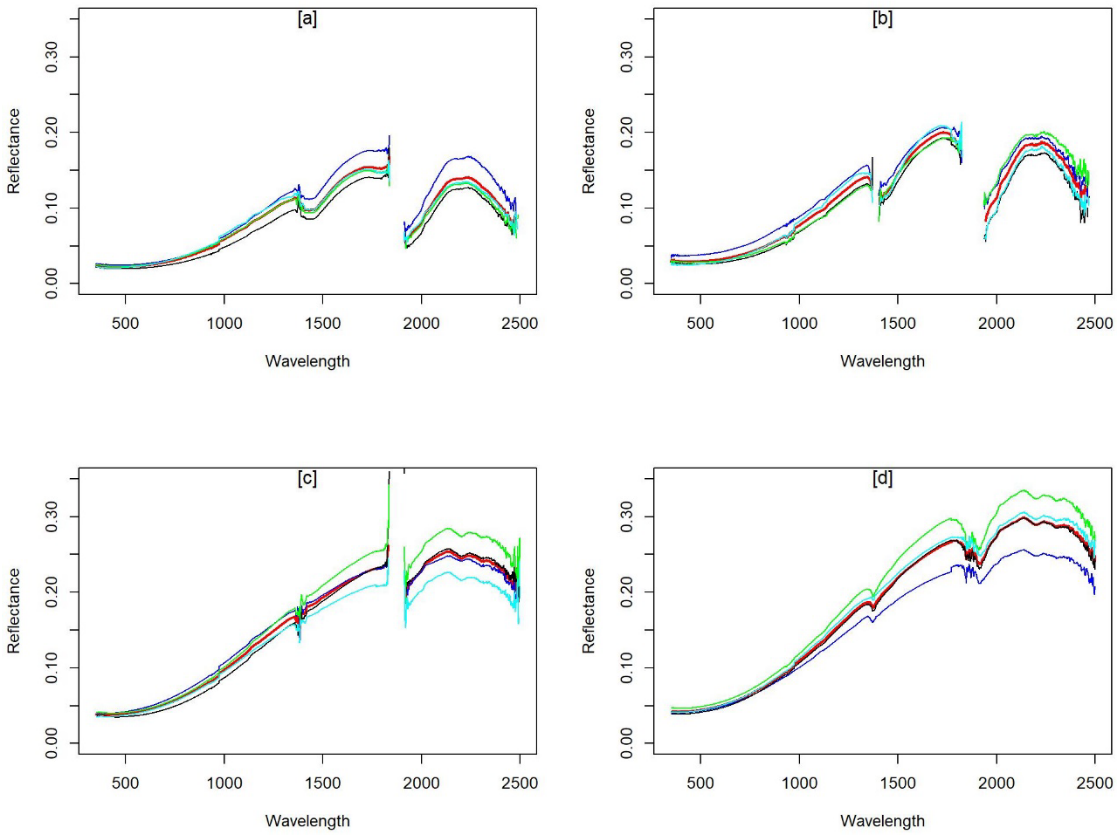

Figure 3.3: Peat reflectance as a function of four moisture content levels: 80%, 57%, 49% and 29%

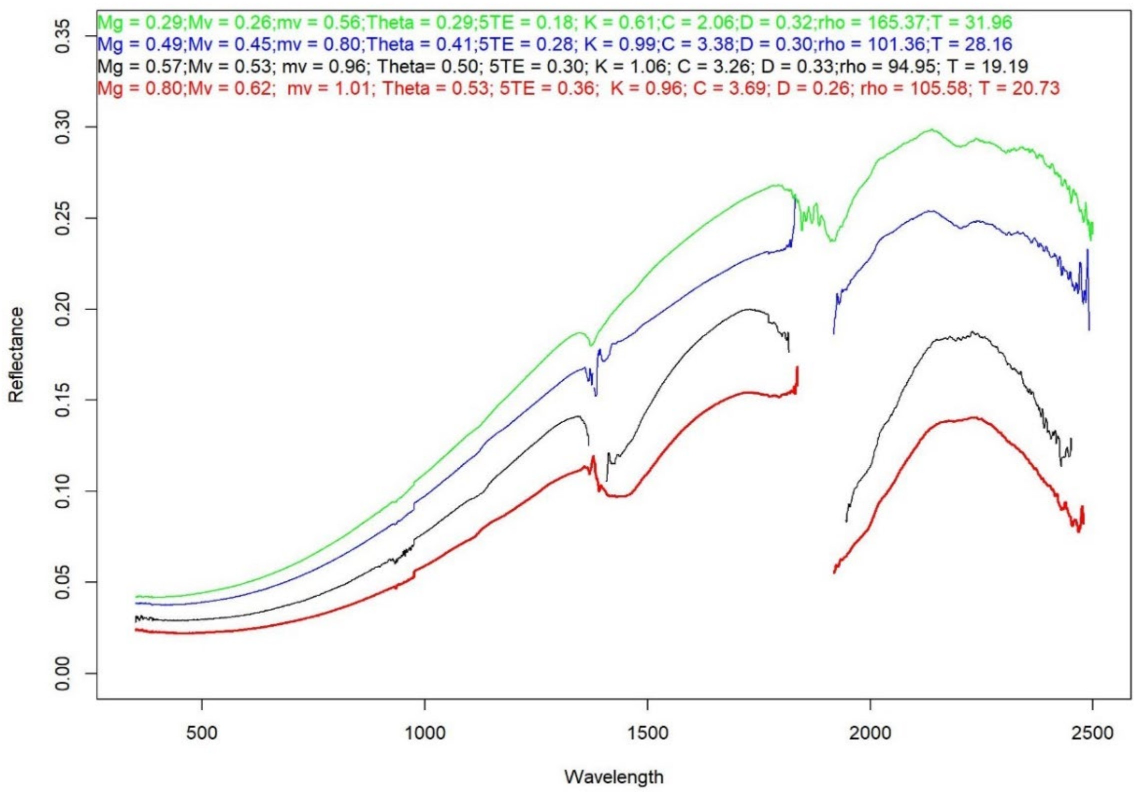

Figure 3.4: Average reflectance at four moisture levels

3.3 EXPERIMENTAL PEAT FIRE DETECTION USING THERMAL INFRARED

The spread of peat fire was relatively slow under the peat surface with an average moisture content (0.262). The peat temperature started to decrease directly after ignition (Figure 3.5). On the other hand, under dry peat conditions (at a moisture content of 0.009), the temperature was relatively high and continued to spread at a very slow rate (Figure 3.6). However, in both cases, the peat fire did not spread over long distances as expected. This can be attributed to the oxygen level within the peat, which suggests that other gases, emitted under natural conditions, may play a big role in how the peat fire spreads or develops downwards and laterally (Huang et al., 2015; Hu, et al., 2018; Huang and Rein, 2019).

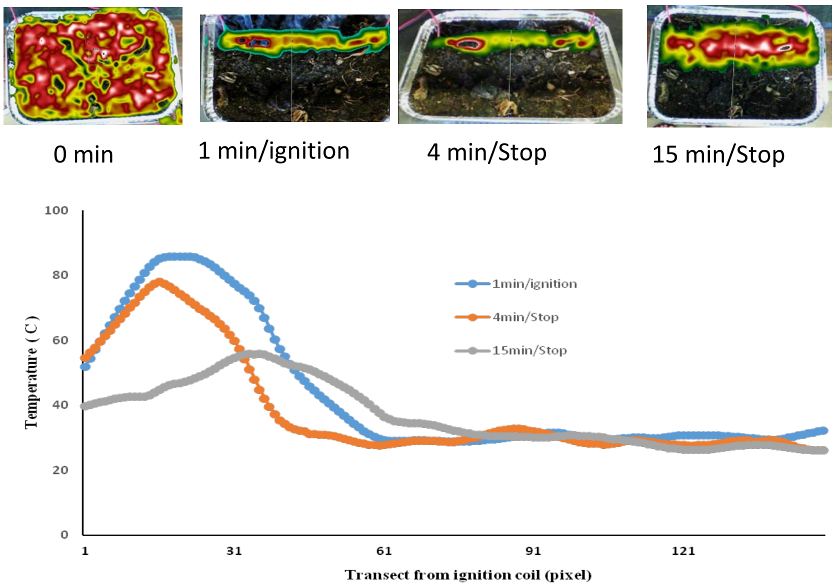

Figure 3.5: *Peat fire spread rate monitored using TIR techniques at laboratory scale (θ = 0.262)*

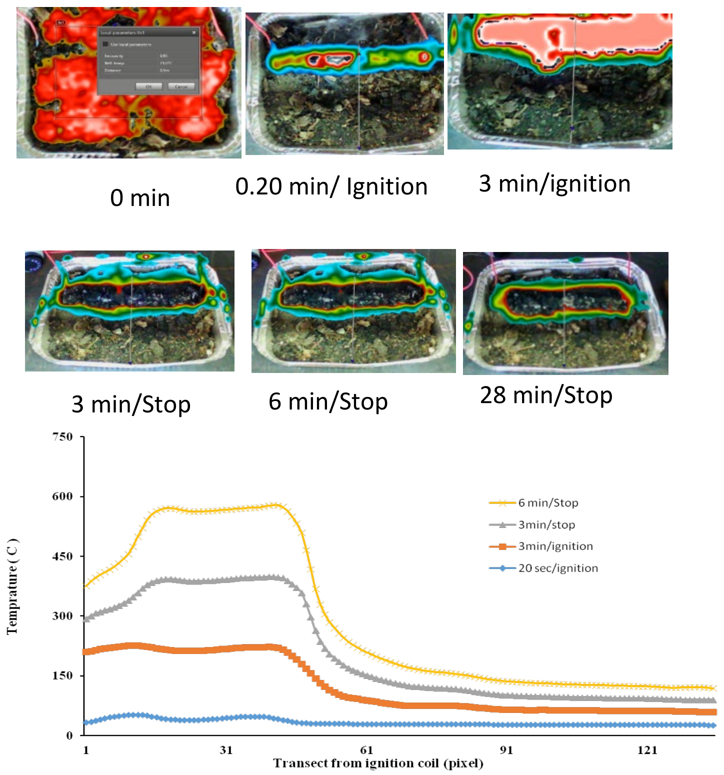

Figure 3.6: *Peat fire spread rate monitored using TIR techniques at laboratory scale (θ = 0.009)*

3.4 DEVELOPMENT OF A PEAT FIRE DETECTION FRAMEWORK

Peat fire, as a phenomenon, is scale dependent. The monitoring techniques must thus be dynamic in the same nature. In other words, the data platform will change with the required monitoring scale (Figure 3.7).

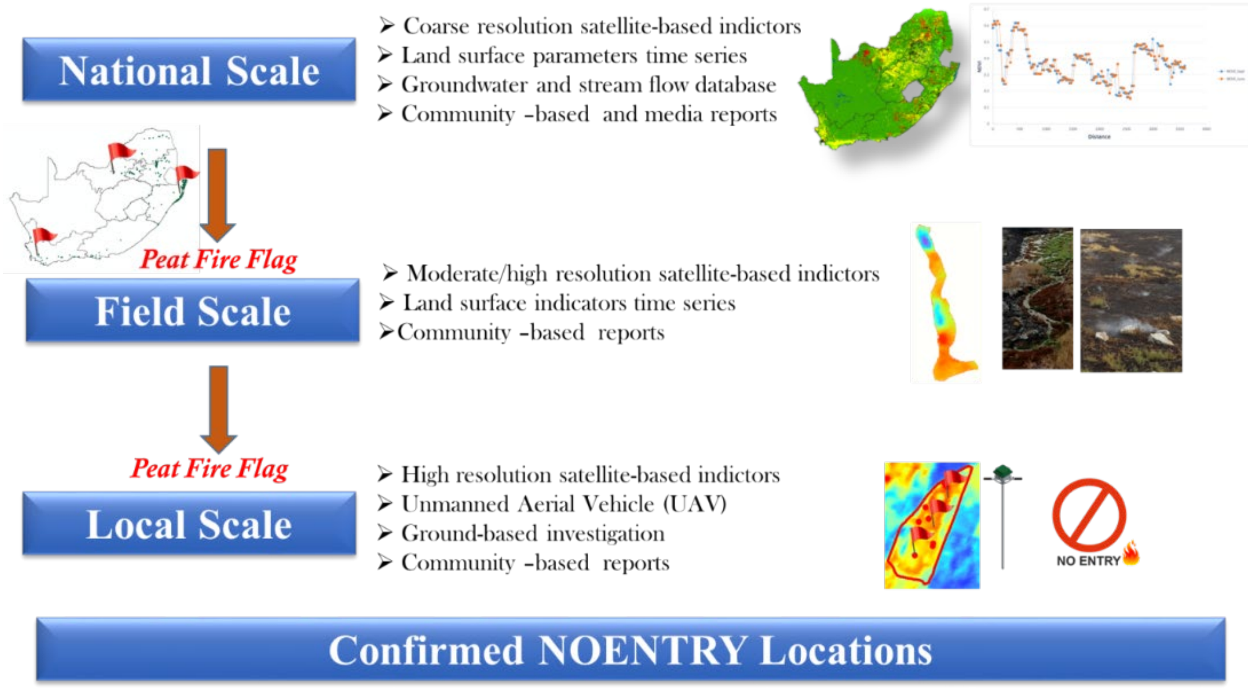

Figure 3.7: Schematic diagram indicating the relationship between monitoring scales and platforms

The national-scale data source included hydrological indicators and time series data extracted at peat locations. Peatlands in South Africa are characterised as small or long linear features in the landscape (e.g. the peat systems in North West), making it difficult to spatially analyse the entire systems on a national scale at the same time. At national scale, it will be suitable to consider the temporal changes at point and small polygon scale for each peatland system and to utilise the long time series to detect the migration from "normal" as an indicator of either negative (degradation) or positive (restoration). The second level is the specific field scale, which can be covered using moderate and high-resolution images. Additionally, time series for land surface indicators can be developed for the area at different locations, combined with spatially distributed indicators (maps). The third level is the local scale, which needs to confirm areas affected by peat fire and to specify smouldering areas (i.e. high risk for no entry), used for guiding and controlling purposes (e.g. fire extinguishing).

The developed framework is shown in Figure 3.8. The development of the framework has considered the four concerns mentioned in section 2.4.

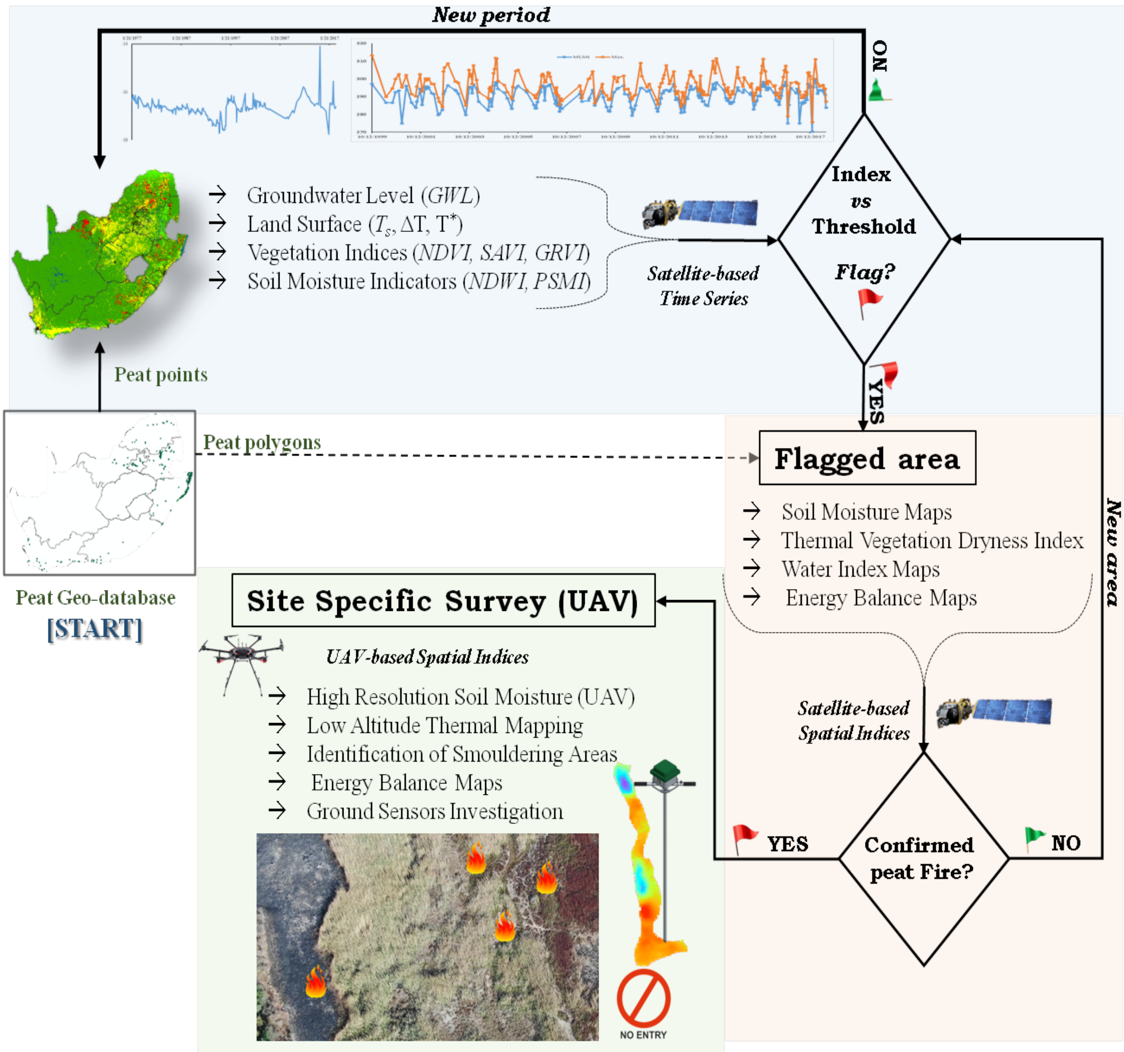

Figure 3.8: Peat fire detection and monitoring framework

The framework design has been divided into three major components: the detection of time series anomalies, satellite-based spatial indices of fire flagged areas, and site-specific assessment using low-altitude sensors. The basic characteristic of the framework is its simplicity and cost effectiveness. The framework will rely mainly on the national peat and groundwater level database, and free available satellite databases in the periodical assessments. The continuous monitoring of the peat systems can be achieved by ranking the peat systems on national scale into classes depending on their susceptibility to dryness and peat fires. The second stage will entail developing automatic groundwater monitoring stations at prioritised systems using Low-Power Wide-Area Networking (LPWAN), for example.

3.5 EXPERIMENTAL PEAT FIRE DETECTION

The peat hotplate experiment aimed to develop indices on a laboratory scale that can be extrapolated to the field. The preliminary results showed high potential to use the changes in spectral signatures as indicators of plant stress due to heat. However, there is a need to verify these indices under different wetting conditions to ensure the stability of the developed indices. The spectral signature of the peat plot under sequential heat stress is shown in Figure 3.9. The spectral data showed clear variation with peat dryness in the Near-Infrared (NIR) and Short-Wave Infrared (SWIR) spectral regions (Figure 3.9). Specifically, these two regions were used to calculate the Normalised Difference Water Index.

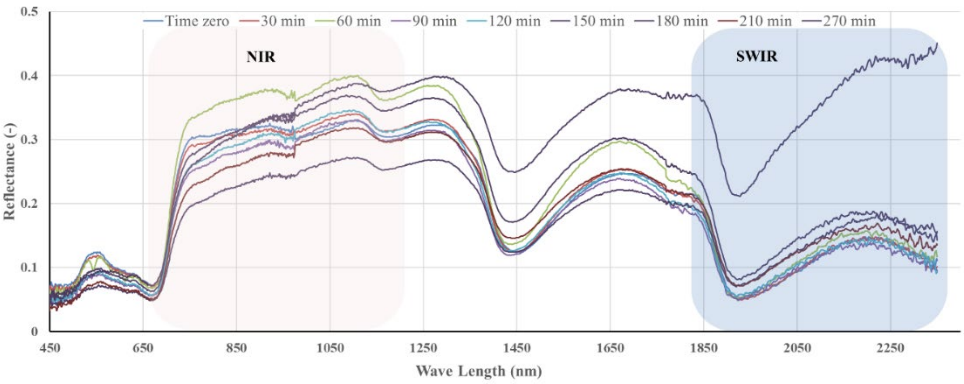

Figure 3.9: *The spectral signature of a peat plot under different time intervals on the hotplate*

3.6 GROUNDWATER MONITORING AS A TOOL FOR PEAT FIRE DETECTION

The groundwater time series can be used as a primary and direct indicator for peat land degradation. The time series of the monthly average groundwater level at three stations close to the three investigated peat systems is shown in Figure 3.10.

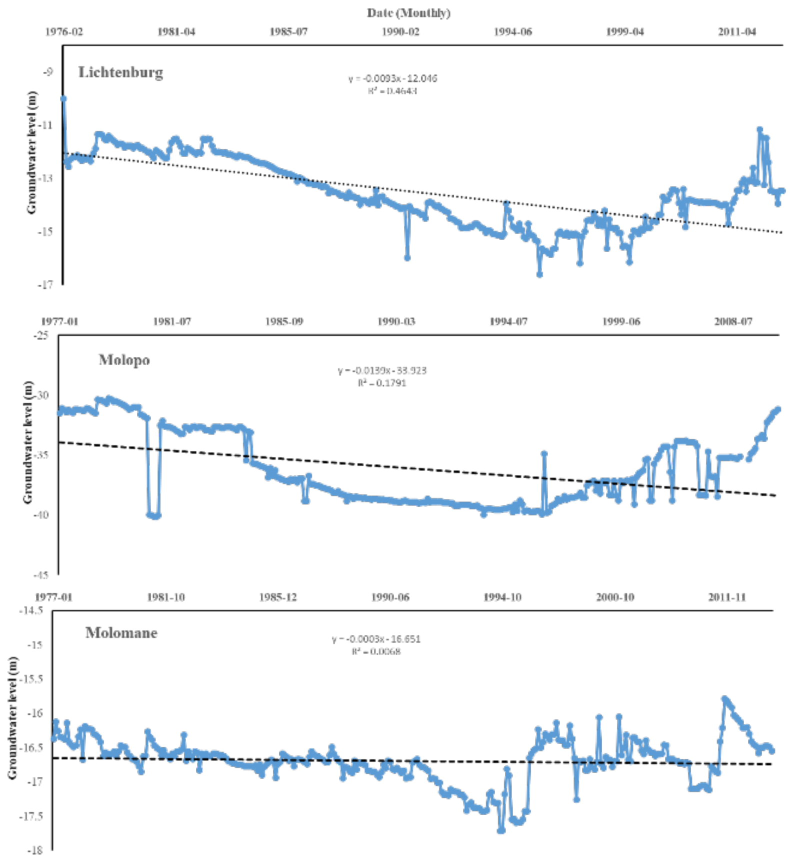

Figure 3.10: *Changes in groundwater level during the last 30 years in three observation wells (the data source is the National Groundwater Archive of the Department of Water and Sanitation)*

The three time series showed clear decreases in groundwater levels in Lichtenburg and Molopo. Considering the degradation and fire incidents in the two systems, there was good agreement between the groundwater trends and reported peat fires. On the other hand, the station close to Molemane showed an approximately stable trend. However, clear fluctuation in groundwater level can be noticed during the last two decades. These fluctuations can be attributed to climatic changes and water abstraction. Although the investigated observation wells were located approximately within the regional groundwater basin, the trends have an agreement with the peat degradation stages. The ideal condition is to have monitoring stations within the peat system to measure rapid responses to groundwater fluctuation in the system. For example, analysis of the diurnal fluctuation in groundwater level can give an indication of the interaction between surrounding land use and hydrology scenarios at the peat system.

Understanding seasonal variation in the groundwater can also help to understand the recharge and discharge periods (Figure 3.10). The drastic decrease in the groundwater level in all seasons in the period between 1986 and 1996 suggests the anthropogenic effect of water abstraction (Figure 3.11).

Figure 3.11: Separation of the seasonal variation in groundwater fluctuation in the Lichtenburg system

3.7 SATELLITE-BASED TIME SERIES ANOMALIES

As shown in section 3.5, spectral signatures proved to be a good indicator of peat dryness in the NIR and SWIR spectral regions. Figure 3.12 shows the temporal changes in the Normalised Difference Water Index (NDWI) in different sampling polygons in the three investigated peat systems.

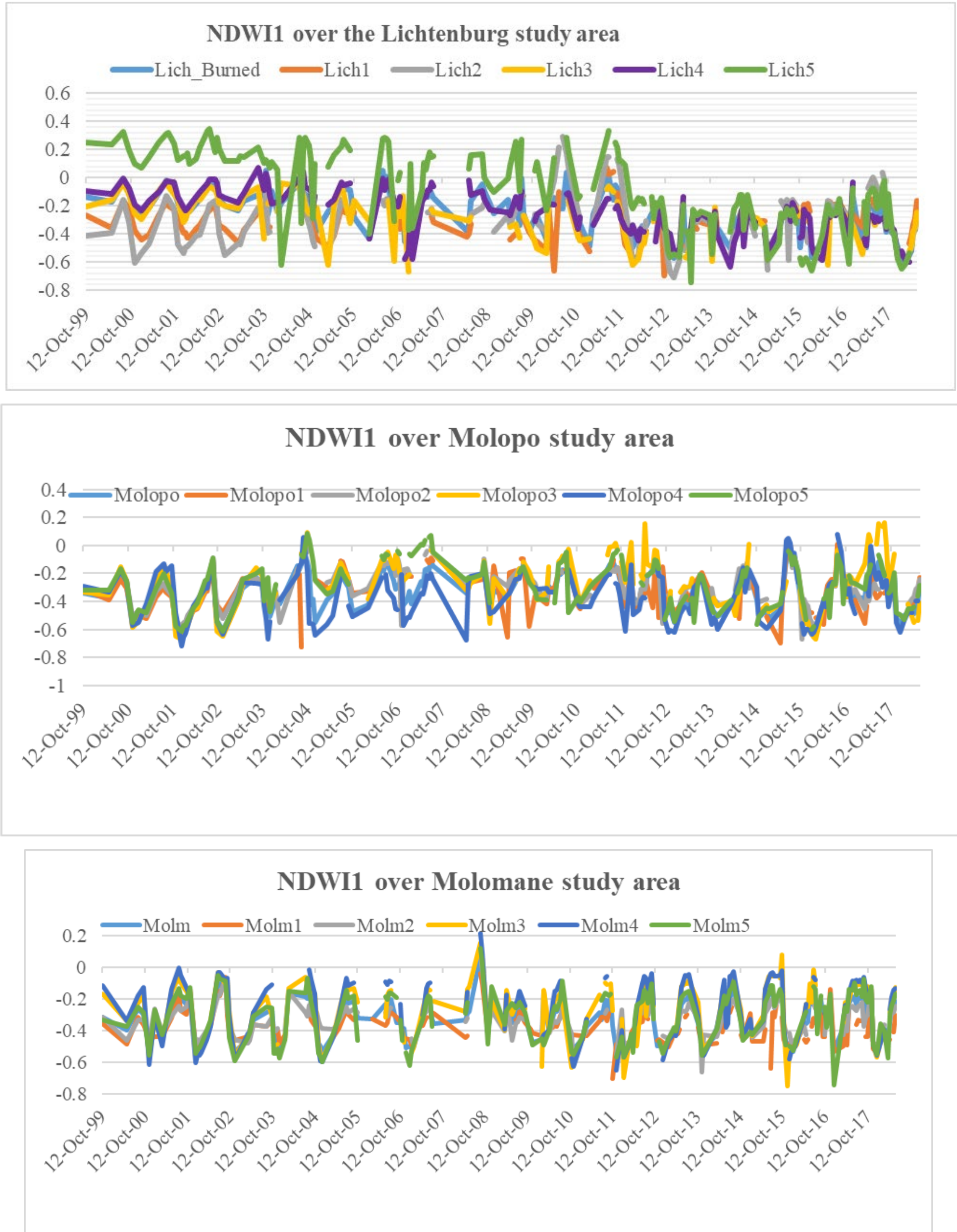

Figure 3.12: Normalised Difference Water Index time series for sampling areas in the Lichtenburg, Molopo and Molemane peat systems

The NDWI showed clear decreases in the Lichtenburg peat system in the period after 2011 (Figure 2.10). Peat fires have been reported in the period between 2013 and 2014. This can support the use of the long-term time series data to indicate anomolies and deviations from normal conditions. The NDWI information can be linked to the land surface temperature retreived for Landsat 7 and 8. The decrease in NDWI can be linked, to a high extent, to the increase in land surface temperature in the Lichtenburg peat system in the same period (Figure 3.13). The same trend can be identified in the Molopo system in the period between 2015 and 2016, which correlates to a peat fire incident that was reported in this period.

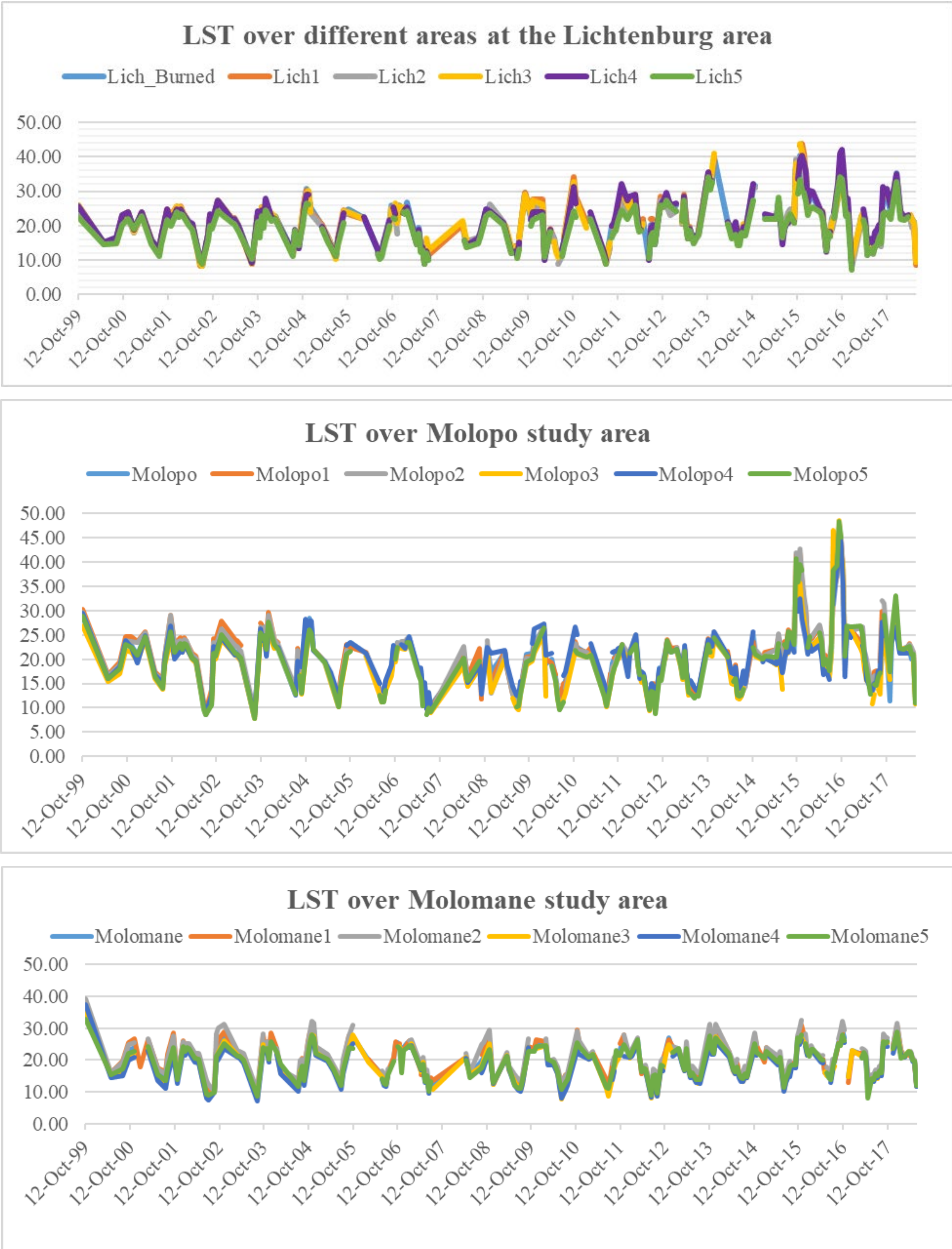

Figure 3.13: Land surface temperature in degrees Celsius at the three peat systems

The magnitude of the NDVI and vegetation indices in general can be affected by vegtation stresses (biotic or abiotic) to various limits (Figure 3.14). However, peat fires are different as the fire fuel is not comprised of photosythetically active meterials compared to wildfires (flaming fires). Due to the saturation and sensitivity effects of the NDVI, it is not recomended to use the NDVI as an indicator for peat fires.

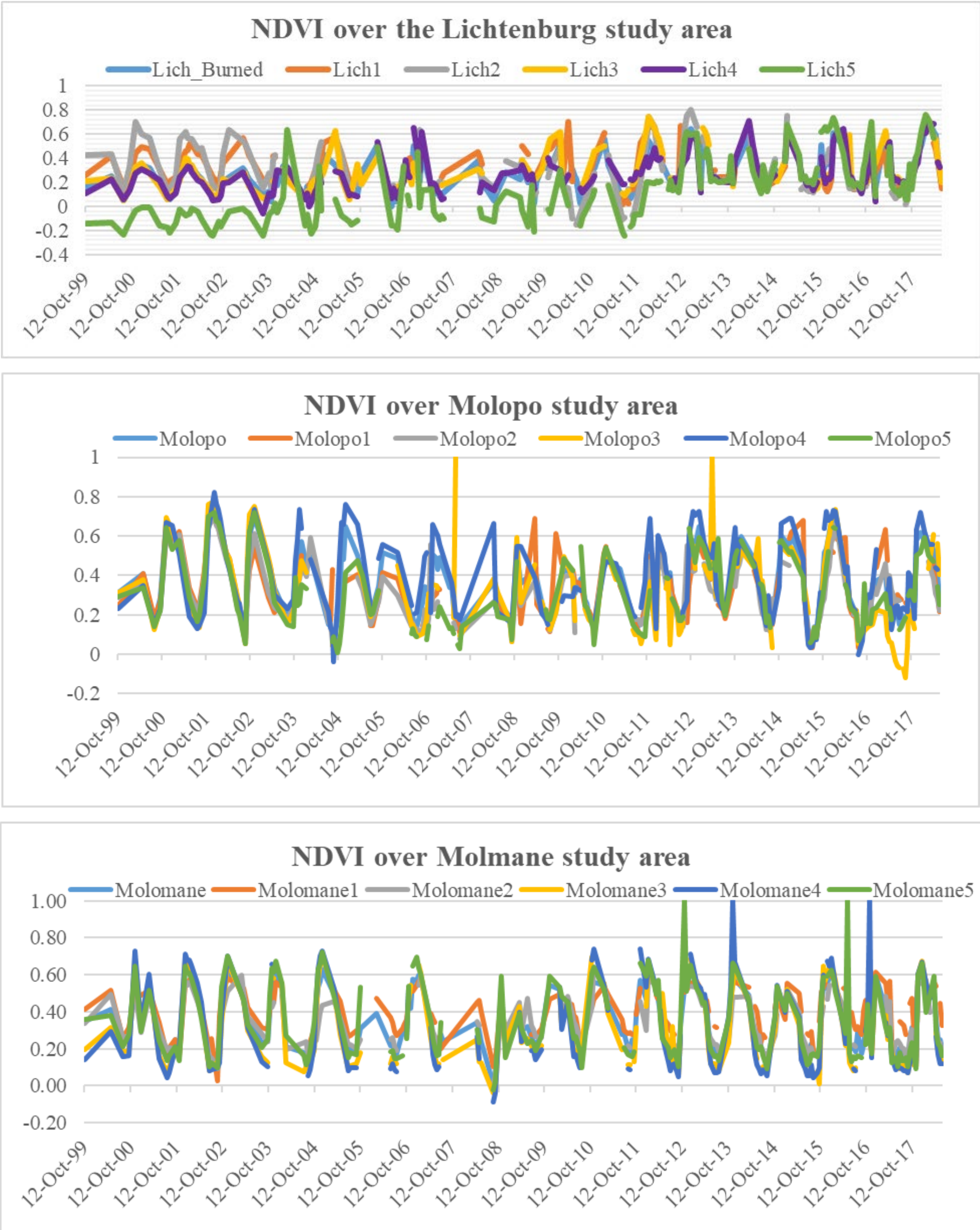

Figure 3.14: The Normalised Difference Vegetation Index for the three research sites

3.8 SATELLITE-BASED SPATIAL ANALYSIS

A small model was developed to calculate different satellite-based, spatially distributed indices (Figure 3.15). The model can be divided into three components: optical indices, thermal indices and combined indices (Figure 3.15). The optical component calculates the vegetation and water indices, whereas the thermal indices determine the surface thermal properties using two thermal bands of Landsat 8. The combined indices aimed to develop plant stress and soil moisture indicators. The input bands can be modified based on the satellite sensors needed. It is suggested that a user interface be developed to assist researchers to develop spatial indicators for different periods. The SMI is a combination between normalised thermal (T_{norm}) data and vegetation cover (renormalised between 0 and 1). The SMI is similar to the Temperature Vegetation Dryness Index (TVDI) in terms of the development concept and has an inverse relationship with soil moisture.

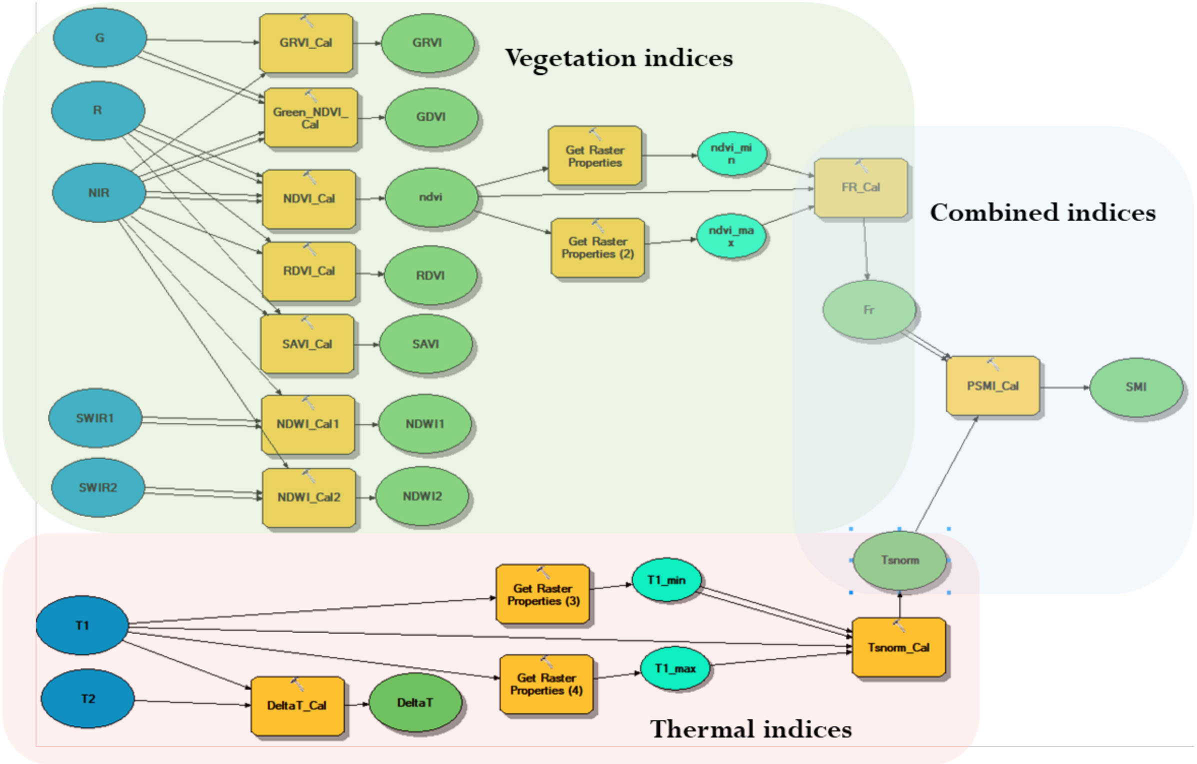

Figure 3.15: Spatial model for satellite-based indices for peat fire assessment

The Lichtenburg research site showed a clear delineation of the water areas with agreement between the SMI (Figure 3.16). The SMI can be compared to the NDVI for the three areas where the open water will show lower NDVI values (Figure 3.17).

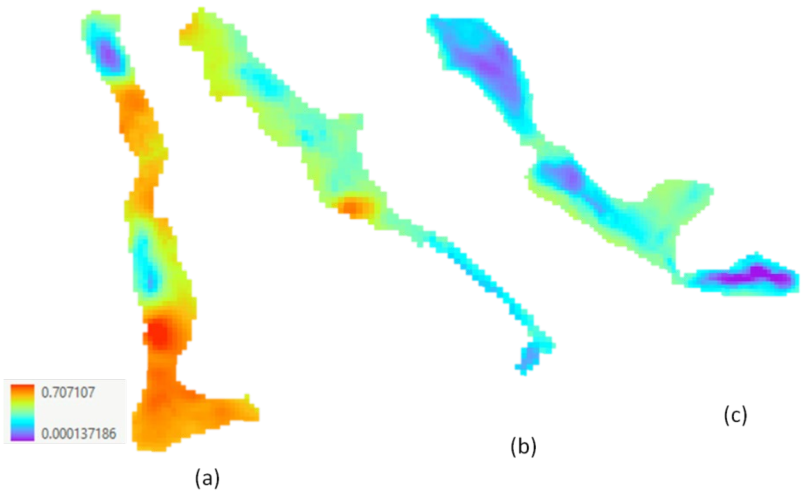

Figure 3.16: The SMI retrieved from a combination between optical and thermal Landsat 8 data at the three sites: (a) Lichtenburg; (b) Molopo; and (c) Molemane

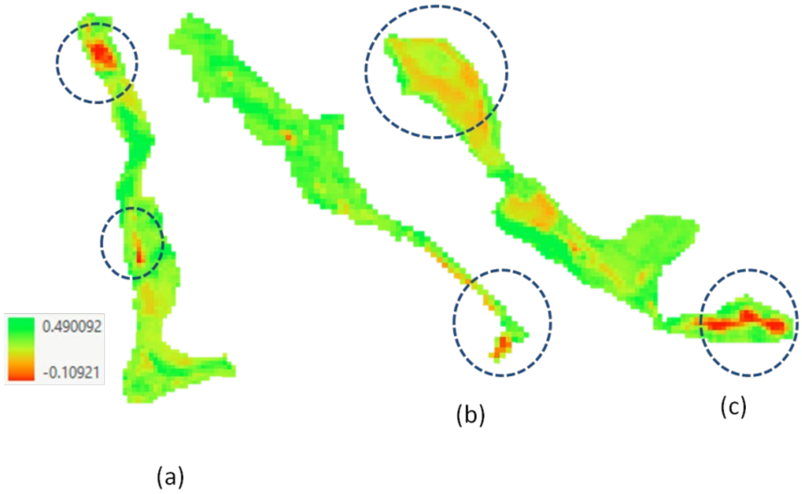

Figure 3.17: The Normalised Difference Vegetation Indext at the three sites: (a) Lichtenburg; (b) Molopo; and (c) Molemane

3.9 UTILISATION OF UNMANNED AERIAL VEHICLES

The combination of optical and thermal remote sensing can produce various indicators that can be related to the surface moisture of the peat surface. The thermal camera and multispectral camera were tested on a laboratory scale. The camera can produce high spatial-resolution images that can detect minor differences on the ground.

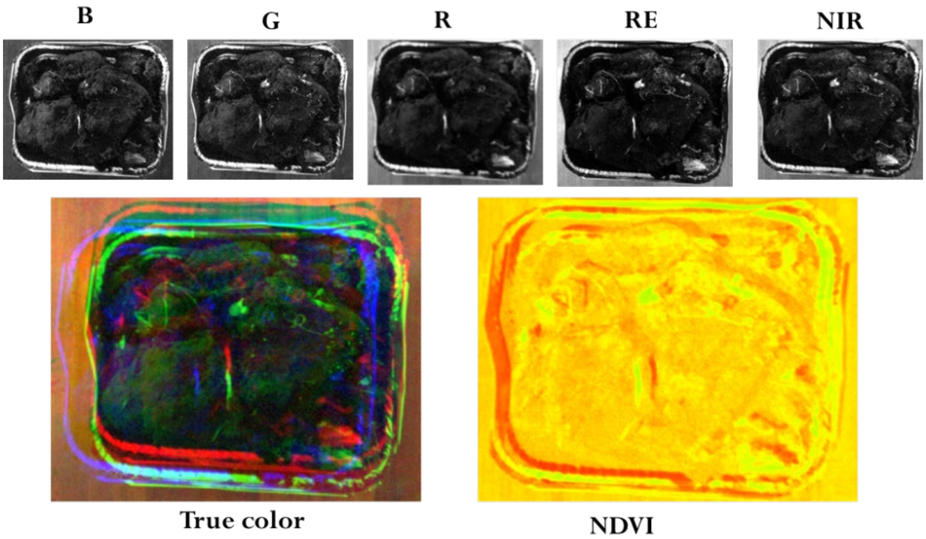

Figure 3.18: Multispectral camera that will be mounted on a UAV system for peat monitoring

3.10 SOIL MOISTURE AND PEAT THERMAL CHARACTERISTICS

The soil moisture and thermal characteristics of two peat systems (Figure 3.19) were monitored at 37 locations (Table 3.3). The average peat moisture at the Molopo site was 0.14 compared to 0.43 at the Molemane site. This is a strong indicator that the Molopo site is undergoing severe dryness. Considering the rainfall experienced during 2019 being deemed normal, the dryness of the peatlands can be attributed mainly to the groundwater abstraction and alteration of natural water flow to the system. The peat dryness can be considered an early warning for the occurrence of fires. However, this condition becomes valid if the peatland has considerable organic matter. The Molopo peatland had historical burning, leaving most of the area covered with a large amount of ash.

The thermal characteristics of the peat were measured in the morning to detect any thermal anomalies. The average temperature was 11.57 °C. The minimum temperature was 7.8 °C and was recorded on bare surface areas. On the other hand, the average surface temperature at the Molemane peatland was 17.75 °C, which was measured during the drone flight around midday. The minimum temperature was 13.12 °C measured at the reeds (*Phragmites australis*) site.

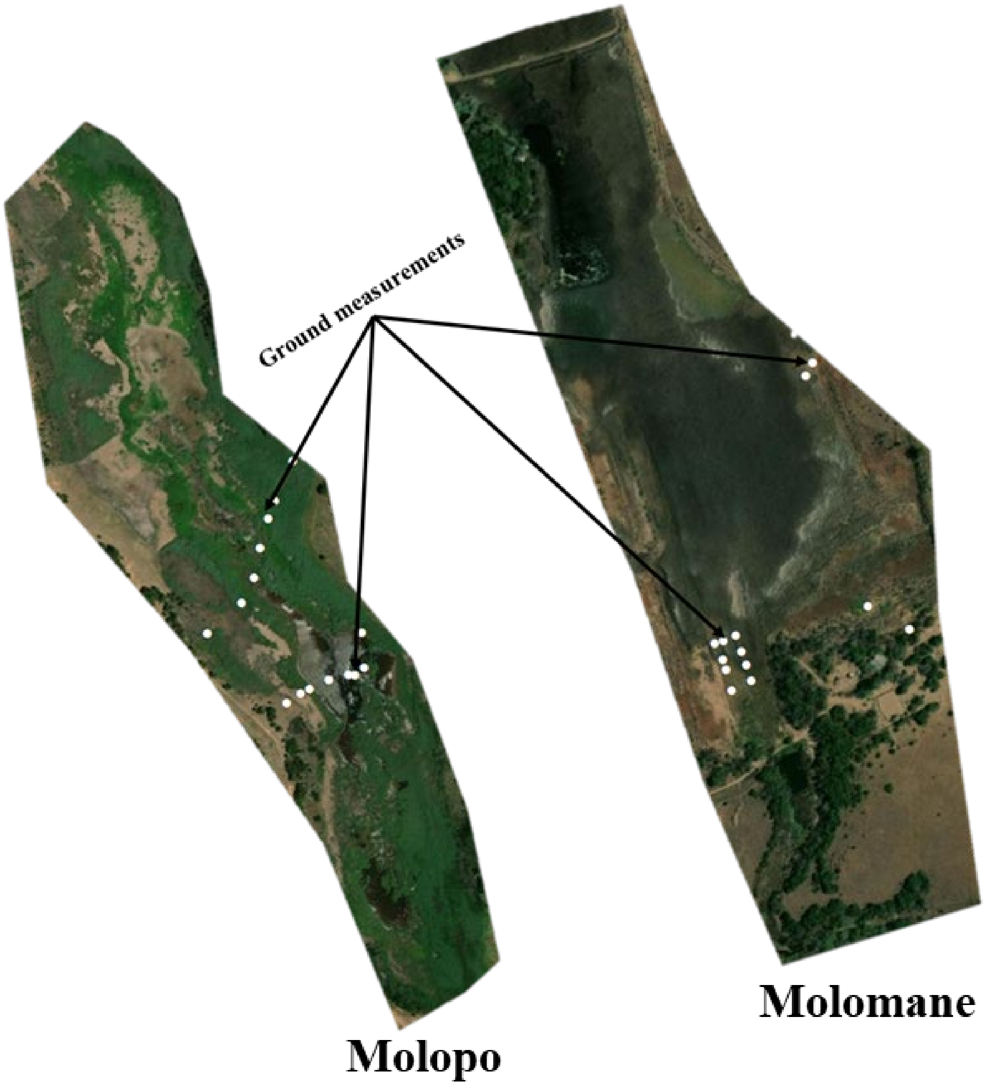

Figure 3.19: Ground measurements of peat moisture and thermal characteristics at the two peatland systems

Table 3.3: Peat moisture and thermal characteristics at the Molopo and Molemane sites

ID	Theta	mv	Rho	T	K	C	D
Molopo							
001	0.26	0.518	198.1	9.94	0.505	1.872	0.27
002	0.226	0.455	351.9	9.38	0.284	1.442	0.197
003	0.2	0.408	177.8	7.39	0.563	2.012	0.28
004	0.088	0.201	459	8.41	0.218	1.07	0.204
005	0.088	0.202	779.1	11.25	0.128	0.666	0.193
006	0.109	0.239	331.9	11.05	0.301	1.225	0.246
007	0.121	0.263	327.1	9.53	0.306	1.561	0.196
008	0.057	0.145	783.3	23.44	0.128	0.94	0.136
009	0.151	0.317	127.1	11.81	0.787	1.681	0.468
010	0.065	0.16	710.6	13.32	0.141	0.947	0.149
011	0.129	0.277	449.5	12.43	0.222	1.259	0.177
012	0.133	0.285	321.9	16.06	0.321	1.331	0.241
013	0.243	0.487	372.4	14.89	0.269	1.491	0.18
014	0.207	0.42	296.3	11.65	0.338	1.753	0.192
015	0.124	0.267	409.9	11.75	0.244	1.452	0.168
016	0.077	0.179	586	9.51	0.171	0.981	0.174
017	0.106	0.234	307.3	8.6	0.325	1.725	0.189
018	0.083	0.266	295	7.85	0.339	1.432	0.237
Molemane							
019	0.524	1.003	183.6	19.61	0.545	2.825	0.193
020	0.569	1.089	148	13.12	0.676	3.946	0.171
021	0.496	0.953	86.72	14.43	1.153	3.089	0.373
022	0.192	0.392	392	19.7	0.255	0.508	0.502
023	0.452	0.872	316.6	28.31	0.316	0.347	0.91
024	0.57	1.089	145.7	19.1	0.686	1.327	0.517
025	0.023	0.139	321.8	30.35	0.311	1.54	0.202
026	0.329	0.783	238	19.1	0.42	1.696	0.248
027	0.046	0.125	748	22.83	0.134	0.668	0.2
028	0.115	0.331	99.11	16.11	1.009	1.193	0.846
029	0.569	1.087	79.94	13.35	1.251	3.276	0.382
030	0.478	0.921	73.78	17.64	1.355	3.621	0.374
031	0.505	0.969	110.2	15.62	0.907	2.807	0.323
032	0.508	0.974	165.4	15.19	0.605	2.873	0.21
033	0.471	0.907	103.6	13.85	0.965	2.613	0.369
034	0.482	0.926	107.6	16.21	0.93	2.867	0.324
035	0.502	0.963	101	13.08	0.99	2.943	0.336
036	0.52	0.996	112.1	14.81	0.992	2.981	0.299
037	0.512	0.981	104.8	14.9	0.955	2.746	0.348

3.11 UAV IMAGES FOR THE TWO SITES

The two peat sites were surveyed using a UAV system that included multispectral and thermal imaging. The image resolution for the optical sensor was 0.04 m for the Molopo and Molemane sites (figures 3.20a and 3.20b), which has been resampled to 0.5 m to assess various indices before the development of the final products.

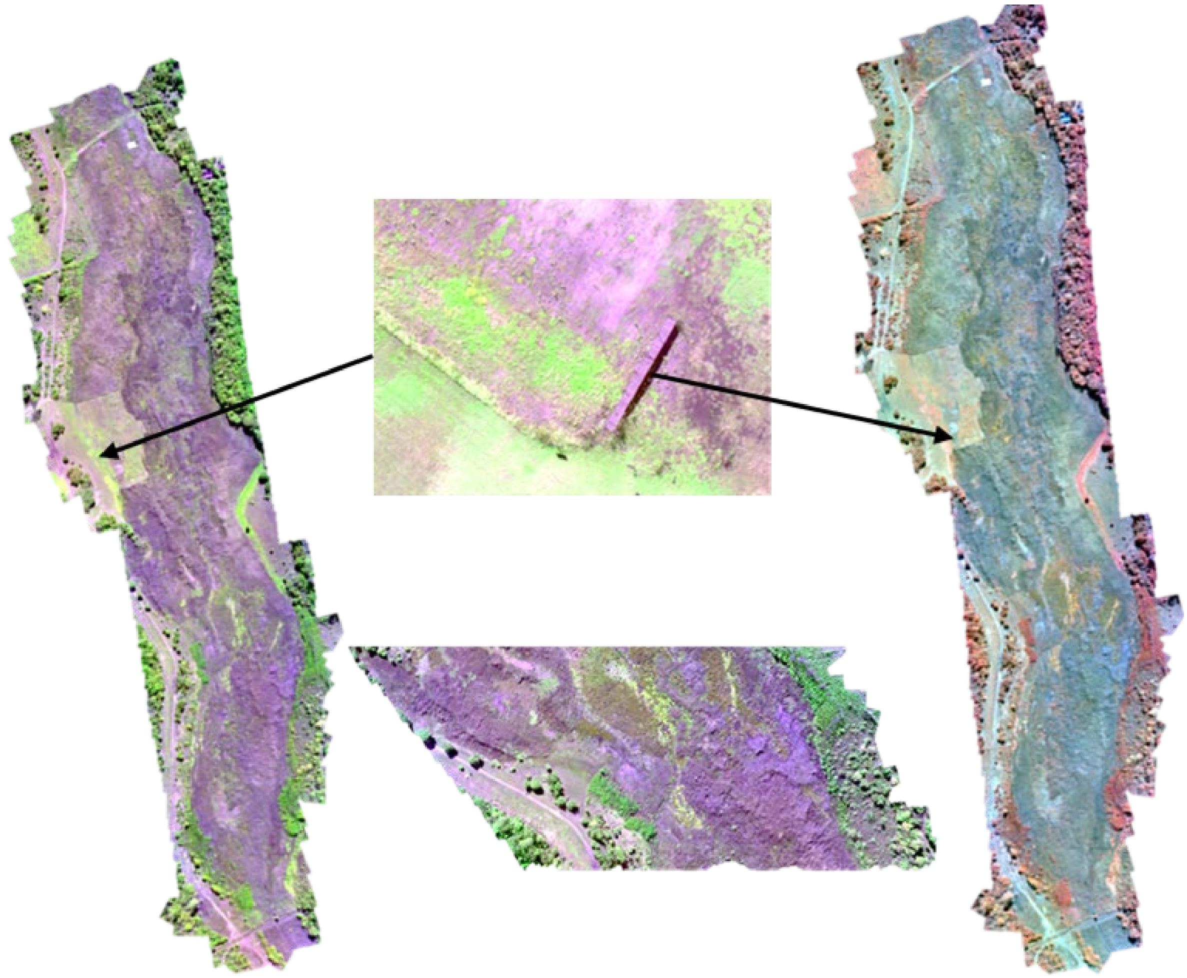

(a)

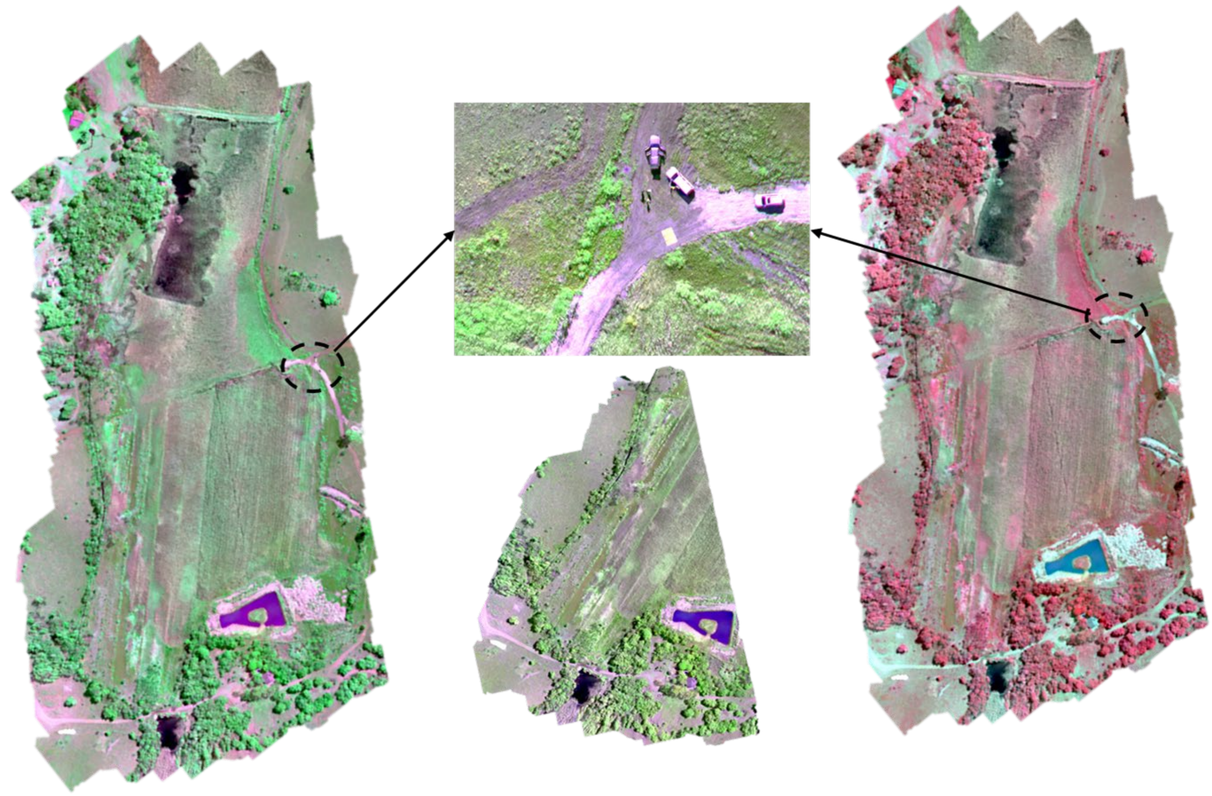

(b)

Figure 3.20: High-resolution multispectral image for: a) the Molopo site; and b) the Molemane site (RGB: 3, 4, 2 and 4, 3, 2).

The image resolution showed high potential to provide the relevant decision makers with the exact location and conditions of the peat and vegetation. The false colour composites clearly showed that the Molopo site was undergoing degradation, as the increase in the red colour indicates healthy and active growing vegetation on the site. The images clearly show the disapperance of free water at the surface of the Molopo peatland compared to Molemane and the historical image shown in Figure 3.19.

3.12 THERMAL IMAGE PROCESSING

Thermal images captured on the UAV platform are a new area of research and development, specifically for images captured for the purpose of determining absolute temperature rather than relative heat. The images were captured using a FLIR® Vue Pro R (13 mm) camera. The absolute temperature was calibrated using single-image analysis on the FLIR® Tool (Figure 3.21).

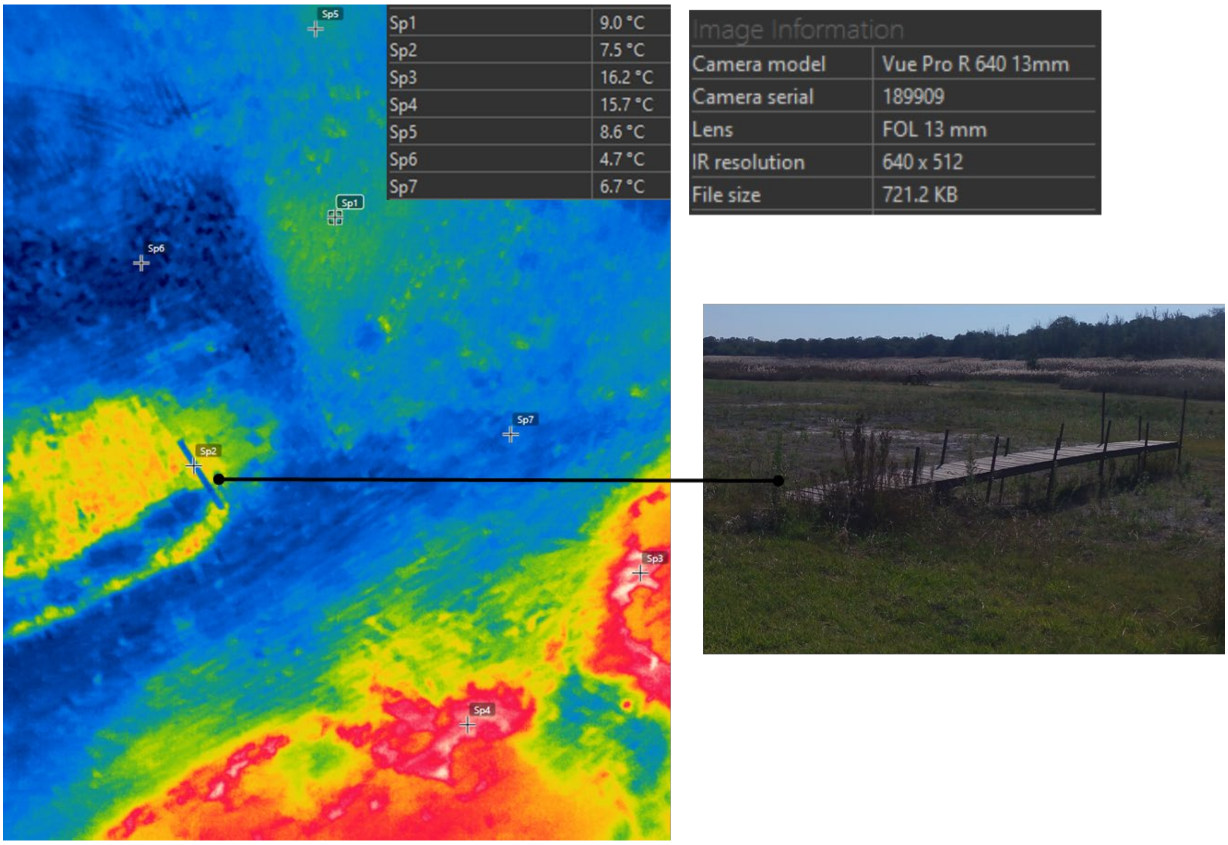

Figure 3.21: Thermal image analysis using the FLIR® Tool for the calibration of absolute temperature

Surface temperature can be interpreted in various directions, the most direct being to detect thermal anomalies, which can be related to fire or smouldering areas. Alternatives include the use of thermal information as a proxy to identify inundated areas. Low temperatures can be outlined and related to high moisture areas in the Molopo peat system (Figure 3.22). On the other hand, the low-temperature areas can be directly linked to the wet areas, water bodies and open water surfaces in the Molemane peat system (Figure 3.23).

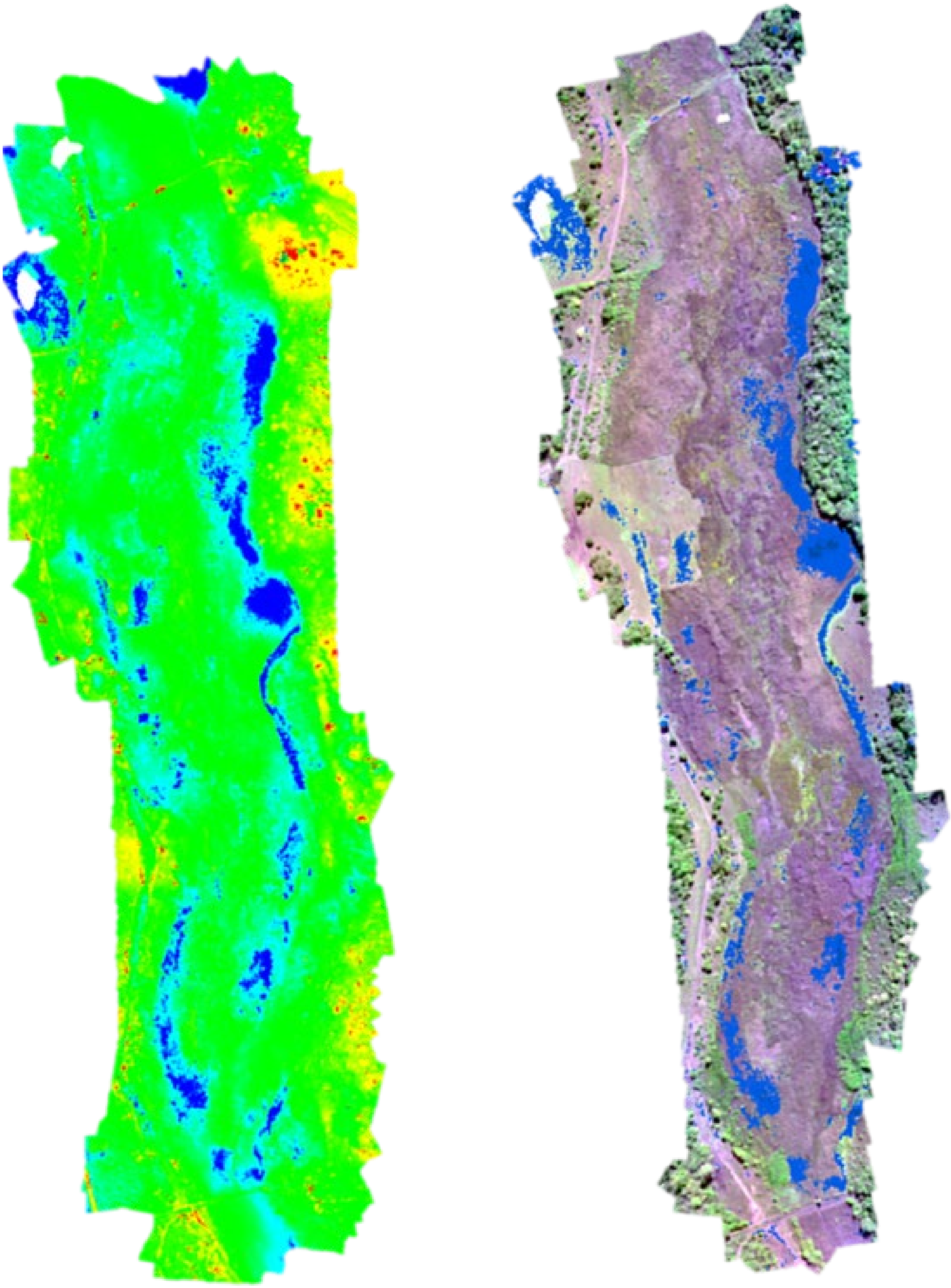

Figure 3.22: The thermal distribution and low-temperature pattern at the Molopo peat system

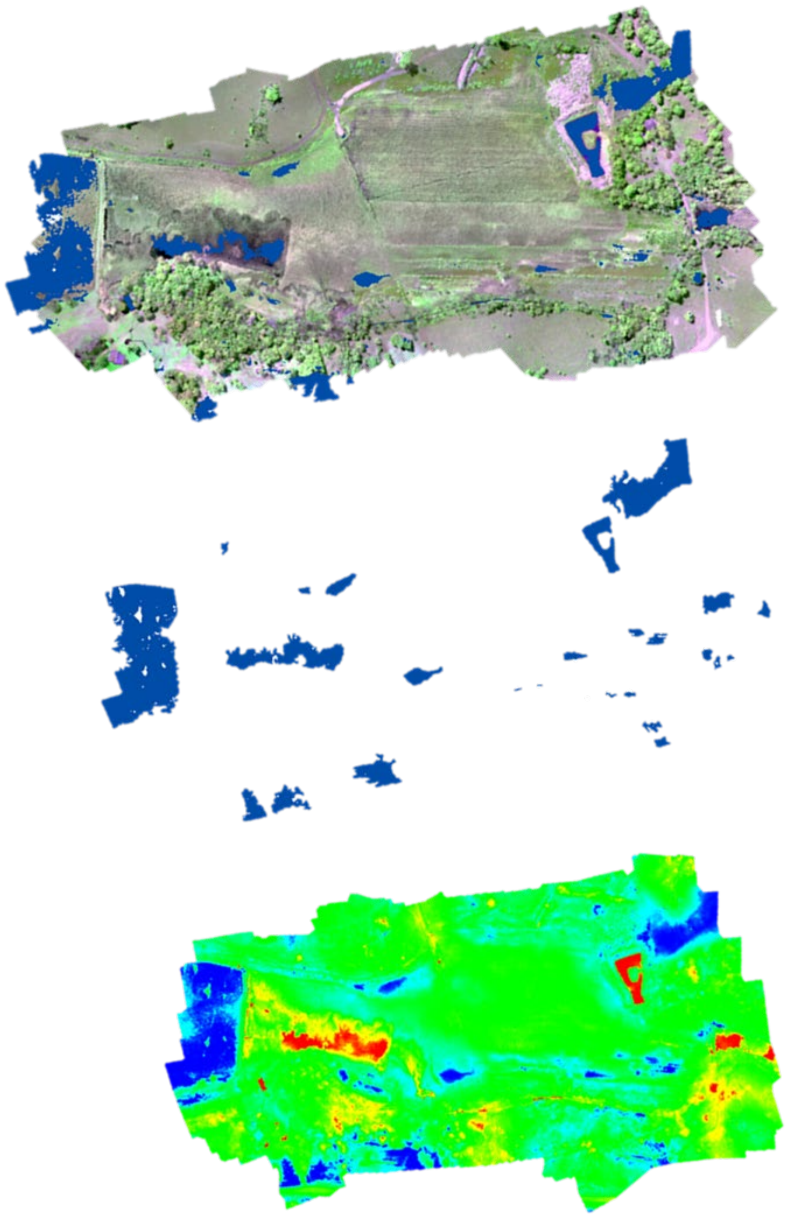

Figure 3.23: The thermal distribution in relationship to free water surfaces and inundation at the Molemane peat system

CHAPTER 4: CONCLUSIONS AND RECOMMENDATIONS

4.1 CONCLUSIONS

Peat soil moisture can be effectively monitored using dielectric sensors with high accuracy. For accurate measurements, the sensors are in need of recalibration as they are mainly designed for mineral soils. The thermal properties of the peat samples have significant association with the peat's moisture levels. This association can also be used to evaluate the peat moisture level on different scales. Peat fires have a series of complex processes that affect the accuracy of the relatively small-scale laboratory simulations. The rate of peat fires is very slow and is highly affected by the moisture levels of the peat. The peat-emitted gases are expected to play a major role in the spreading of peat fires along the big cracks. These cracks formed when the peat dried and allowed an increase of oxygen in the lower layers.

Images from the UAV platform were captured. The images were successfully processed at these stages and the mosaicked images generated. The size of the image was reduced to assess various indices and peat degradation indicators. At this stage, none of the two sites showed any thermal anomalies. However, the Molopo peatland is experiencing severe dryness, making the remaining peat susceptible to fire.

The developed framework has various components that range between *in situ* ground measurements, low-altitude sensors and satellite-based indicators. Peat fires consist of multiple processes and factors that interact with each other to make the peatland systems susceptible to fire. These factors include natural/climatic and anthropogenic factors.

Studying the three sites that varied from completely dry and degraded (Lichtenburg) to a wet and functional system (Molemane), one could clearly see that the Lichtenburg site experienced a reduction in the water table based on the groundwater level analysis. The satellite-based time series showed strong signals related to the wetting condition and weak signals regarding the peat fire periods in Lichtenburg and Molopo. The high variability within the pixels led to minimising the peaks. This might suggest the use of more robust sampling techniques to ensure the ability to capture minimal changes in the system temperature. The validation stages (i.e. experimental determination of peat thermal and moisture relationships) were important for the peat fire monitoring framework's indicators selection. However, the above-normal rainy season in 2018/19 might influence the expected number of peat fire incidents anticipated across the country.

4.2 RECOMMENDATIONS

The main aim of the study was to develop a peat fire monitoring framework based on the integration of various data sources. Based on the research findings, the following recommendations and future prospects for research are made:

- The role of the methane gas emission on peat fire processes and acceleration should be determined.
- The framework relies on peat "points" and peat "polygons". It is therefore necessary to have detailed studies that verify all peat sites and delineate these systems.
- Groundwater monitoring systems should be developed to update the peat monitoring framework with continuous and frequent groundwater-level data.
- An investment should be made in future research work to operationalise the framework at national or provincial level. The advantage for the operationalisation of the monitoring framework is to apply an automated peat fire monitoring system that automatically couples groundwater levels and anomalies detected from satellite-based information.

- It is suggested that the framework be hosted by the Department of Human Settlements, Water and Sanitation as the main custodian of ground and surface water information. However, the detection of peat fires can also be important for several directorates in the Department of Environmental Affairs, Forestry and Fisheries, and the Department of Agriculture, Land Reform and Rural Development.

Peat Fire Workshop

Peatlands are under increasing threat from agriculture, mining and infrastructure development. Authorities should take extra precautions to prevent peat degradation and peat fires, which occur underground. Peat fires are of major concern, especially in the timber industry, and an urgent request was aired for a peat fire workshop. The aim of this workshop is to bring authorities, environmentalists and the timber industry together to explain where and why peat fires occur, as well as to share the results of this study on how and if remote sensing could be used as an effective tool in natural resources monitoring and management. Wetlands, and specifically peatlands, are valuable natural resources that need to be electively monitored and managed. One of the needs expressed is how to control and rehabilitate the peat fires in the short term and how to manage the problem in the long term.

REFERENCES

ADINUGROHO WC, I NYOMAN N. SURYADIPUTRA, BAMBANG H. SAHARJO, and LABUENI SIBORO. 2005. *Manual for the control of fire in peatlands and peatland forest.* Climate Change, Forests and Peatlands in Indonesia Project, Wetlands International – Indonesia Programme and Wildlife Habitat Canada, Bogor, Indonesia.

ANSHARI GZ, AFIFUDIN M, NURIMAN M, GUSMAYANTI E, ARIANIE L, SUSANA R, NUSANTARA RW, SUGARDJITO J and RAFIASTANTO A (2010). Drainage and land use impacts on changes in selected peat properties and peat degradation in West Kalimantan Province, Indonesia. Biogeosciences **7** 3403–3419.

BAILEY AK and PITMAN WV (2012) *Water resources of South Africa, 2012 Study (WR2012)*. WRC Report No. TT 754/1/18, Water Research Commission, Pretoria, South Africa.

BECKER F and LI ZL (1990) Temperature-independent spectral indices in thermal infrared bands. Remote Sensing of Environment **32** 17–33.

CANCELLIERI V, CANCELLIERI D, LEONI E, SIMEONI A and FILKOV A (2014) Energetic potential and kinetic behavior of peats. Journal of Thermal Analysis and Calorimetry **117** 1497–1508.

DASH P, GOTTSCHE FM, OLESEN FS and FISCHER H (2002) Land surface temperature and emissivity estimation from passive sensor data: Theory and practice – current trends. International Journal of Remote Sensing **23** 2563–2594.

DEPARTMENT OF WATER AFFAIRS AND FORESTRY (DWAF) (2010) *North West Groundwater Master Plan* (NWGMP). DWAF, Pretoria, South Africa.

DRYSDALE D (1998) *An introduction to fire dynamics*, 2nd ed., Wiley, Chichester, UK.

DRYSDALE D (2011) *An Introduction to fire dynamics*, 3rd ed., Wiley, Chichester, UK.

ELVIDGE CD, ZHIZHIN M, HSU F-C, BAUGH K, KHOMARUDIN MR, VETRITA Y, SOFAN P, SUWARSONO and HILMAN D (2015) Long-wave infrared identification of smouldering peat fires in Indonesia with nighttime Landsat data. Environmental Research Letters **10 (6)** 065002.

ESRI (2020) ArcMap™ 10 software, 2011. www.esri.com.

FILKOV A, SINYUTKINA A and KHARANZHEVSKAYA Y (2015) Geoinformation system for prediction of peat fires and its validation. In: *International Multidisciplinary Scientific GeoConference Surveying Geology and Mining Ecology Management*.

FRANCA GB and CRACKNELL AP (1994) Retrieval of land and sea surface temperature using NOAA-11 AVHRR data in north-eastern Brazil. International Journal of Remote Sensing **15** 1695–1712.

FRANÇOIS C and OTTLÉ C (1996) Atmospheric corrections in the thermal infrared: Global and water vapor dependent split-window algorithms-applications to ATSR and AVHRR data. IEEE Transactions on Geoscience and Remote Sensing **34** 457–470.

FRIEDL MA (2002) Forward and inverse modelling of land surface energy balance using surface temperature measurements. Remote Sensing of Environment **79** 344–354.

GILLESPIE AR (1985) Lithologic mapping of silicate rocks using TIMS. In: *Proceedings of the TIMS Data User's Workshop,* ABBOTT EA, 29–44, Jet Propulsion Laboratory, Pasadena, CA, USA.

GILLESPIE AR, ROKUGAWA S, MATSUNAGA T, COTHERN JS, HOOK SJ and KAHLE AB (1998) A temperature and emissivity separation algorithm for advanced spaceborne thermal emission and reflection radiometer (ASTER) images. IEEE Transactions on Geoscience and Remote Sensing 36 1113–1126.

GRUNDLING P (2011) Peat fires in southern African peatlands. WETREST Report 2011/07/101.

GRUNDLING P (2002) *The quaternary peat deposits of Maputaland, northern KwaZulu-Natal, South Africa.* Master's dissertation, University of Johannesburg, Johannesburg, South Africa.

GRUNDLING P, GRUNDLING AT, PRETORIUS L, MULDERS J and MITCHELL S (2017) *South African peatlands: Ecohydrological characteristics and socio-economic value.* WRC Report No. 2346/1/17, Water Research Commission, Pretoria, South Africa.

GRUNDLING P, MAZUS H and BAARTMAN L (1998) *Peat resources in northern KwaZulu-Natal wetlands: Maputaland*. Department of Environmental Affairs and Tourism, Pretoria, South Africa.

GRUNDLING P, PRICE JS, GROOTJANS AP and ELLERY WN (2013) *The capability of the Mfabeni peatland to respond to climatic and land-use stresses, and its role in sustaining discharge to downstream and adjacent ecosystems.* WRC Report No. 1857/1//12, Water Research Commission, Pretoria, South Africa.

GRUNDLING PL and BLACKMORE A (1998) *Peat fire in the Vasi Pan Peatland: Manzenwenya plantation.* Report No. 1998-0208, Council for Geoscience, Pretoria, South Africa.

GRUNDLING P-L and MARNEWECK G (1999) *Mapping, characterisation and monitoring of the Highveld.* WRC Report No. 2346/1/17, Water Research Commission, Pretoria, South Africa.

GRUNDLING P-L and MARNEWECK G (2000) Proposed rehabilitation of the railway at the poort section in the Colbyn Valley Wetland (Slope Failure at 8,8 km Hartbeesfontein – Koedoespoort), Preliminary Wetland Study, Wetland Consulting Services (Pty.) Ltd., Reference: COL 01/35/2000.

GRUNDLING P-L (2018) Personal communication: Piet-Louis Grundling, Deputy Director: Programme

GRUNDLING P-L and GROBLER R (2005) Peatlands and mires of South Africa. Stapfia **35** 379–396.

GUMBRICHT T, MCCARTHY TS, MCCARTHY J, ROY DP, FROST PE and WESSELS K (2002) Remote sensing to detect sub-surface peat fires and peat fire scars in the Okavango Delta, Botswana. South African Journal of Science **98** 351–360.

HOLDEN J and BURT TP (2003) Hydrological studies on blanket peat: The significance of the acrotelm-catotelm model. Journal of Ecology **91** 86–102.

HOOIJER A, PAGE S, JAUHIAINEN J, LEE WA, LU XX, IDRIS A and ANSHARI G (2012) Subsidence and carbon loss in drained tropical peatlands. Biogeosciences **9** 1053–1071.

HOOK SJ, GABELL AR, GREEN AA and KEALY PS (1992) A comparison of techniques for extracting emissivity information from thermal infrared data for geologic studies. Remote Sensing of Environment **42** 123–135.

HU Y, FERNANDEZ-ANEZ N, SMITH TEL and REIN G (2018) Review of emissions from smouldering peat fires and their contribution to regional haze episodes. International Journal of Wildland Fire **27** 293–312.

HUANG X and REIN G (2019) Upward-and-downward spread of smoldering peat fire. Proceedings of the Combustion Institute **37** 4025–4033.

HUANG X, REIN G and CHEN H (2015) Computational smouldering combustion: Predicting the roles of moisture and inert contents in peat wildfires. Proceedings of the Combustion Institute **35** 2673−2681.

JOOSTEN H (2010) *The global peatland CO_2 picture: Peatland status and drainage related emissions in all countries of the world.* Countries of the World, Wetlands International, Ede, The Netherlands.

JOOSTEN H and CLARKE D (2002) *Wise use of mires and peatlands: Background and principles including a framework for decision-making.* International Mire Conservation Group and International Peat Society.

KAHLE AB, MADURA DP and SOHA JM (1980) Middle infrared multispectral aircraft scanner data: Analysis for geological applications. Applied Optics **19** 2279−2290.

KEALY P and HOOK S (1993) Separating temperature and emissivity in thermal infrared multispectral scanner data: Implication for recovering land surface temperatures. IEEE Transactions on Geoscience and Remote Sensing **31** 1155−1164.

KEALY PS and GABELL AR (1990) Estimation of emissivity and temperature using alpha coefficients. In: *Proceedings of Second TIMS Workshop,* ABBOTT EA, 11−15, Jet Propulsion Laboratory, Pasadena, CA, USA.

LABBÉ S, LEBOU RGEOIS V, JOLIVOT A and MARTI R (2012) *Thermal infra-red remote sensing for water stress estimation in agriculture.* Options Méditerranéennes B No. 67, 2012 – The use of remote sensing and geographic information systems for irrigation management in Southwest Europe, 175−184.

LAPPALAINEN E (1996) *Global peatland resources.* International Peat Society and Geological Survey of Finland, Jyskä, Finland.

LI Z, BECKER F, STOLL M and WAN Z (1999) Evaluation of six methods for extracting relative emissivity spectra from thermal infrared images. Remote Sensing of Environment **69** 197−214.

LIANG S (2001) An optimization algorithm for separating land surface temperature and emissivity from multispectral thermal infrared imagery. IEEE Transactions on Geoscience and Remote Sensing **39** 264−274.

LYON RJP (1965) Analysis of rocks by spectral infrared emission (8 to 25 micron). Economic Geology **60** 715−736.

MALHERBE J, DIEPPOIS B, MALULEKE P, VAN STADEN M and PILLAY DL (2016) South African droughts and decadal variability. Natural Hazards **80** 657–681.

MALHERBE J, SMITH IPJ, WESSELS KJ and BEUKES PJ (2020) Recent droughts in the Kruger National Park as reflected in the extreme climate index. African Journal of Range and Forage Science **37 (1)** 1–17.

MARNEWECK GC, GRUNDLING PL and MULLER JL (*2001) Defining and classification of peat wetland ecoregions in South Africa*. Wetland Consulting Services (Pty) Ltd. Report to the Institute for Soil, Climate and Water (ISCW), Agricultural Research Council for the Directorate for Land and Resources Management (DLRM), Department of Agriculture, Pretoria, South Africa.

MARTINI IP, CORTIZAS AM and CHESWORTH W (2006) *Peatlands: Evolution and records of environmental and climate changes,* Elsevier, Amsterdam, The Netherlands.

MUCINA L and RUTHERFORD MC (2006) The vegetation of South Africa, Lesotho and Swaziland. Strelitzia **19**, South Africa National Biodiversity Institute, Pretoria, South Africa.

NGIE A, ABUTALEB K, AHMED F, DARWISH A and AHMED M (2014) Assessment of urban heat island using satellite remotely sensed imagery: A review. South African Geographical Journal **96** 198–214.

NORTH WEST DEPARTMENT OF AGRICULTURE, CONSERVATION AND ENVIRONMENT (NWDACE) (2008) *North West Province Environment Outlook.* NWDACE, Mahikeng, South Africa.

PERDANA L, RATNASARI N, RAMADHAN M, PALAMBA P, NASRUDDIN N and NUGROHO Y (2017) Hydrophilic and hydrophobic characteristics of dry peat. IOP Conference Series: Earth and Environmental Science **105**. http:doi.org/10.1088/1755-1315/105/1/012083.

PRADHAN B, BIN SULIMAN MDH and BIN AWANG MA (2007) Forest fire susceptibility and risk mapping using remote sensing and geographical information systems (GIS). Disaster Prevention and Management **16 (3)** 344–352

PRATA AJ, CASELLES V, COLL C, SOBRINO JA and OTTLÉ C (1995) Thermal remote sensing of land surface temperature from satellites: Current status and future prospects. Remote Sensing Reviews **12** 175–224.

PRAT-GUITART N, REIN G, HADDEN RM, BELCHER CM and YEARSLEY JM (2016) Effects of spatial heterogeneity in moisture content on the horizontal spread of peat fires. Science of the Total Environment **572** 1422–1430.

PRICE JC (1984) Land surface temperature measurements from the split window channels of the NOAA 7 advanced very high-resolution radiometer. Journal of Geophysical Research **89** 7231–7237.

QIN Z, KARNIELI A and BERLINER P (2001) A mono-window algorithm for retrieving land surface temperature from Landsat^{TM} data and its application to the Israel-Egypt Border Region. International Journal of Remote Sensing **18** 3719–3746.

REALMUTO VJ (1990) Separating the effects of temperature and emissivity: Emissivity spectrum normalization. In: *Proceedings of the 2nd TIMS Workshop,* ABBOTT EA, 31–37, Jet Propulsion Laboratory, Pasadena, CA, USA.

RESTUCCIA F, HUANG X and REIN G (2017) Self-ignition of natural fuels: Can wildfires of carbon-rich soil start by self-heating? Fire Safety Journal **91** 828–834.

RYDIN H, JEGLUM JK and BENNETT KD (2013) *The biology of peatlands*, Oxford University Press, Oxford, UK.

SANTAMOURIS M, PAPANIKOLAOU N, LIVADA I, KORONAKIS I, GEORGAKIS C, ARGIRIOU A and ASSIMAKOPOULOS DN (2001) On the impact of urban climate to the energy consumption of buildings. Solar Energy **70** 201–216.

SCHMUGGE T, HOOK SJ and COLL C (1998) Recovering surface temperature and emissivity from thermal infrared multispectral data. Remote Sensing of Environment **65** 121–131.

SIEGERT F, ZHUKOV B, OERTEL D, LIMIN S, PAGE SE and RIELEY JO (2004) Peat fires detected by the BIRD satellite. International Journal of Remote Sensing **25 (16)** 3221–3230.

SOBRINO JA and CASELLES V (1991) A methodology for obtaining the crop temperature from NOAA-9 AVHRR data. International Journal of Remote Sensing **12** 2461–2475.

SOBRINO JA, Jiménez-Muñoz JC and Leonardo P (2004) Land surface temperature retrieval from LANDAT^{TM} 5. Remote Sensing of Environment **90** 434–440.

SOBRINO JA, LI ZL, STOLL MP and BECKER F (1994) Improvements in the split window technique for land surface temperature determination. IEEE Transactions on Geoscience and Remote Sensing **32** 243–253.

UNITED NATIONS ENVIRONMENT PROGRAMME (UNEP) (1992) *World atlas of desertification*, UNEP, London, UK.

VAN DEVENTER H, SMITH-ADAO L, JOB N, GENTHE B, GRUNDLING A, GRUNDLING P-L, IMPSON D, KOTZE D, NEL JL, PETERSEN C, ROBINSON J, SCHERMAN P, SIEBEN E, SNADDON K, TERERAI F, VAN DER COLFF D and VAN RENSBURG S (2018) *South African National Biodiversity Assessment 2018. Technical Report. Volume 2: Inland Aquatic (Freshwater) Component.* CSIR Report No. CSIR/NRE/ECOS/IR/2018/0001/A; SANBI Report No. SANBI/NAT/NBA2018/2019/Volx/A, South African National Biodiversity Institute, Pretoria, South Africa.

WAN Z, ZHANG Y, ZHANG Q and LI Z (2002) Validation of the landsurface temperature products retrieved from terra moderate resolution imaging spectroradiometer data. Remote Sensing of Environment **83** 163–180.

WATSON K (1992) Spectral ratio method for measuring emissivity. Remote Sensing of Environment **42** 113–116.

WETLAND CONSULTING SERVICES (PTY) LTD (n.d.) *Peatlands: Compilation of existing data and evaluation of inventory methodology.* WCS Report No: 28/99, report to the Institute for Soil, Climate and Water (ISCW), Agricultural Research Council for the Directorate for Land and Resources Management (DLRM), Department of Water, Agriculture and Forestry, Pretoria, South Africa; Water Research Commission, Pretoria, South Africa.

WHITFIELD PH, ST-HILAIRE A and VAN DER KAMP G (2009) Improving hydrological predictions in peatlands. Canadian Water Resources Journal **34** 467–477.

WIEDER RK and VITT DH (2006) *Boreal peatland ecosystems*, Springer, Dordrecht, The Netherlands.

WIJEDASA LS (2016) Peat soil bulk density important for estimation of peatland fire emissions. Global Change Biology **22** 2959.

ZHANG J, WANG Y and LI Y (2006) A C++ program for retrieving land surface temperature from the data of Landsat^{TM}/ETM+ band6. Computers and Geosciences **32** 1796–1805.